

1  
2  
3  
4  
5  
6  
7  
8  
9  
10  
11  
12  
13  
14  
15  
16  
17  
18  
19  
20  
21  
22  
23  
24  
25  
26

**A metagenomics pipeline reveals insertion sequence-driven evolution of the microbiota**

Joshua M. Kirsch<sup>1</sup>, Andrew J. Hryckowian<sup>2,3</sup>, and Breck A. Duerkop<sup>1,4</sup>

<sup>1</sup>Department of Immunology and Microbiology, University of Colorado - Anschutz Medical Campus, School of Medicine, Aurora, Colorado, 80045, USA

<sup>2</sup>Department of Medicine, Division of Gastroenterology and Hepatology, University of Wisconsin School of Medicine and Public Health, Madison, Wisconsin, 53706, USA

<sup>3</sup>Department of Medical Microbiology & Immunology, University of Wisconsin School of Medicine and Public Health, Madison, Wisconsin, 53706, USA

<sup>4</sup>Lead Contact: Breck A. Duerkop, [breck.duerkop@cuanschutz.edu](mailto:breck.duerkop@cuanschutz.edu)

## 27 **Abstract**

28 Insertion sequence (IS) elements are mobile genetic elements in bacterial genomes that support  
29 adaptation. We developed a database of IS elements coupled to a computational pipeline that  
30 identifies IS element insertions in the microbiota. We discovered that diverse IS elements insert  
31 into the genomes of intestinal bacteria regardless of human host lifestyle. These insertions  
32 target bacterial accessory genes that aid in their adaptation to unique environmental conditions.  
33 Using IS expansion in *Bacteroides*, we show that IS activity leads to insertion “hot spots” in  
34 accessory genes. We show that IS insertions are stable and can be transferred between  
35 humans. Extreme environmental perturbations force IS elements to fall out of the microbiota and  
36 many fail to rebound following homeostasis. Our work shows that IS elements drive bacterial  
37 genome diversification within the microbiota and establishes a framework for understanding how  
38 strain level variation within the microbiota impacts human health.

39

## 40 **Introduction**

41 Bacteria rapidly evolve their genomes through the mobilization of genetic elements,  
42 including bacteriophages (phages), plasmids, DNA inversions, and transposable elements<sup>1-3</sup>.  
43 Genetic rearrangements have a strong impact on bacterial fitness, influencing diverse  
44 phenotypes including virulence, antibiotic resistance, interbacterial competition, and secondary  
45 metabolism. For example, pathogenicity islands can distribute virulence traits to previously non-  
46 pathogenic bacteria and DNA inversions can alter the expression of antibiotic resistance  
47 genes<sup>4,5</sup>. Additionally, novel genetic traits such as metabolic and virulence genes are acquired  
48 by bacteria through plasmid exchange, bacteriophage lysogeny, and conjugative  
49 transposition<sup>6,7</sup>. Thus, mobile elements actively drive bacterial adaptation and evolution.

50 Insertion sequence (IS) elements are small (~1 kB) simple transposons that are  
51 common to bacterial genomes<sup>8</sup>. IS elements are capable of self-mobilization by activating an  
52 encoded transposase that recognizes sequence-specific inverted repeats at IS element termini.

53 IS transposases are diverse<sup>9</sup>, and include enzymes with a DD(E/D) motif that support “copy-  
54 and-paste” and “cut-and-paste” mechanisms or those with HUH nuclease chemistry which  
55 transpose as ssDNA molecules at the replication fork<sup>10-12</sup>. Gene expression and genome fidelity  
56 can be modulated by IS activity in a variety of ways, including IS insertions into protein coding  
57 sequences inactivating genes, insertions into intergenic regions forming strong hybrid promoters  
58 increasing gene expression, or recombination with other IS elements resulting in large  
59 deletions<sup>13-16</sup>. Additionally, IS elements can rapidly expand in bacterial genomes when  
60 commensal bacteria transition to become pathogens<sup>15,17,18</sup>. Thus, IS elements have a profound  
61 impact on the evolution and physiological traits of bacteria<sup>19</sup>.

62 Despite a deep knowledge of fundamental IS biology from diverse bacteria, we have a  
63 rather rudimentary understanding of how these elements function in polymicrobial communities.  
64 This knowledge is critical for deciphering how bacterial communities evolve in ecosystems such  
65 as the human microbiota. A barrier to studying IS elements in complex environments result from  
66 imperfect methodologies for measuring *in situ* IS element dynamics. This stems from the poor  
67 recovery of multi-copy genes with repetitive sequences by short-read assemblers, leading to  
68 fragmented assemblies where IS elements are absent or become break-points between  
69 contigs<sup>20</sup>. Therefore, assembly-level analyses of IS elements from metagenomic datasets are  
70 often underpowered. Despite these limitations, previous culture-based studies show that IS  
71 elements are active in the human intestine. Sampling of *Bacteroides fragilis* isolates revealed  
72 the gain and loss of IS transposases<sup>21</sup>. Furthermore, IS elements were shown to rapidly expand  
73 in copy number in the genome of *Escherichia coli* during intestinal colonization of mice, driving  
74 increased virulence in a mouse model of Crohn’s disease<sup>22,23</sup>. Recently, longitudinal intestinal  
75 metagenomic samples from a single individual were sequenced using long DNA fragment  
76 partitioning, producing higher quality assemblies compared to short-read methodologies. This  
77 analysis revealed that *Bacteroides caccae* gained and lost numerous IS insertions over the  
78 course of sampling<sup>20</sup>. Finally, we previously utilized a targeted IS sequencing approach to

79 identify insertions of the IS element IS256 in intestinal *Enterococcus faecium* populations  
80 isolated from an individual undergoing treatment with multiple antibiotics<sup>19</sup>. Antibiotic exposure  
81 was associated with increased abundances of IS256 insertions in genes related to antibiotic  
82 resistance and virulence, suggesting that antibiotic treatment drives IS-mediated  
83 pathoadaptation in the human intestine.

84 In this work, we developed an open-source IS database that greatly expands the  
85 diversity of IS elements compared to current databases. We built a computational pipeline that  
86 utilizes this database to find IS insertions in public metagenomic datasets. Our analysis reveals  
87 widespread abundance and expansion of IS insertions in the human microbiota. We show that  
88 IS insertions are transferable between individuals and are stable for years. Distinct families of IS  
89 elements are favored for insertional activity within the microbiota and these preferentially insert  
90 into specific classes of genes. Such genes are linked to distinct microbial taxa with an  
91 overrepresentation within the *Bacteroidia* and *Clostridia*. Gene classes targeted by IS elements  
92 are primarily metabolic, cell surface, and mobile genetic element genes. Using an *in vitro*  
93 ISOSDB412 (IS4351) expansion model, we confirm that identical and related accessory genes  
94 are preferentially targeted. Finally, we show that the stability of IS insertions is lost following  
95 antibiotic perturbation and diet intervention. Following these alterations, new IS abundances and  
96 insertion site locations arise. Together, this work establishes a framework for studying IS  
97 elements within the microbiota and is the first step toward understanding how IS elements  
98 contribute to the function of the microbiota impacting human health.

99

## 100 **Results**

### 101 ***ISOSDB: a comprehensive open-source IS database***

102 To facilitate the study of IS elements in bacterial genomes and metagenomic datasets,  
103 we sought to build an updated and exhaustive IS database that can serve as an open-source  
104 tool for the scientific community. Prior to our development of this database, the main repository

105 for IS elements was the ISFinder database<sup>24</sup>. While ISFinder has served as a gold-standard for  
106 the systematic naming of IS elements and their identification in single isolate genomes<sup>25</sup>, it is  
107 underpowered for high-throughput genomics. ISFinder lacks integration into downstream tools  
108 that can facilitate in-depth analyses of IS elements, the entirety of the database cannot be  
109 downloaded for personal use, and it relies solely on manual curation and submission of new IS  
110 elements, decreasing the speed at which new IS elements can be reported. These are  
111 drawbacks in the current genomic age, where the identification of IS elements from complex  
112 datasets such as metagenomes would greatly improve our understanding of their function.

113 To address the need for an unrestricted open-access IS database to support genomic  
114 research, we built the Insertion Sequences Open-Source Database (ISOSDB), which consists of  
115 IS elements identified from 39,878 complete bacterial genomes and 4,497 metagenome  
116 assembled genomes (MAGs)<sup>26</sup>. These IS elements were identified using OASIS, a rigorously  
117 tested IS identification tool that allows for the high-throughput analysis of multiple genomes<sup>27</sup>. IS  
118 elements were considered valid and included in ISOSDB if: 1) there were at least two copies of  
119 the IS element in a single genome, 2) it was flanked by terminal inverted repeats (IRs), and 3)  
120 has significant nucleotide homology to an IS element in ISFinder or has a putative transposase.  
121 Redundant IS elements were deduplicated at 95% nucleotide identity. The resulting set of IS  
122 elements totaled 22,713 distinct IS elements, an almost five-fold excess to the ISFinder  
123 database (Fig. 1A). We identified transposase amino acid homologs, in addition to nucleotide  
124 homology over the whole sequence of an IS element, in the ISFinder database. 97.5% of the  
125 transposases included in ISOSDB had protein homologs in ISFinder, but only 37.9% had  
126 nucleotide homologs in ISFinder (Fig. 1B). The ISOSDB also has a wide range of transposases  
127 representing multiple IS families and contains distinct clusters of IS elements at the nucleic acid  
128 and protein level (Fig. 1C-D & Table S1). In summary, the ISOSDB is an expansive, freely  
129 available database that contains substantially improved IS diversity compared to current  
130 databases.

131

132 ***Development of an IS detection pipeline that uses ISOSDB***

133 IS elements drive genomic diversity in almost all bacterial species<sup>9,28,29</sup>. However, a  
134 systematic method to identify IS insertions in complex microbial communities has not been  
135 previously developed. This has precluded the study of IS biology in the microbiota at the  
136 population scale. To obtain a deeper understanding of IS biology in the microbiota, we  
137 developed the pseudoR pipeline that utilizes ISOSDB to identify IS insertions in previously  
138 assembled genomic sequences. pseudoR is named for its ability to find IS inactivated  
139 pseudogenes and is implemented in the R programming language. This pipeline is built for  
140 fragmented, incomplete assemblies such as metagenomes. Our approach was inspired by  
141 previous tools developed for the analysis of transposon insertions from eukaryotic<sup>30</sup> and  
142 bacterial genomes<sup>31,32</sup>. These tools either require *a priori* knowledge of target site duplications  
143 which is often not consistent for IS insertions<sup>33</sup>, use read pairing to infer IS insertions which  
144 limits the data available to verify IS insertions, or require a matched reference assembly.

145 The backbone of the pseudoR pipeline is a split read approach. First, reads are mapped  
146 against assembled contigs and unmapped reads are binned as separate read files. These  
147 unmapped reads are aligned against a database of IS terminal ends (150 bp on either end of an  
148 IS) compiled from ISOSDB (Fig. S1). If an unmapped read has an IS termini, the termini is  
149 trimmed and the remaining read is remapped against the assembled contigs. To ensure that  
150 insertions are genuine, a minimum depth of four reads is required and these reads must include  
151 at least one left and one right termini.

152 To compare between samples and multiple disparate assemblies, we built two modes  
153 (multi and single). Multi-mode takes each sample and maps its reads against its own assembly.  
154 These reads are then subsequently mapped against a deduplicated gene database built from all  
155 assemblies in the dataset. Single-mode was developed to analyze time series datasets, where a

156 single assembly can be used for multiple samples (such as one from the start of the time  
157 series).

158

### 159 ***IS insertions are widespread in the healthy human intestinal microbiota***

160 We utilized the pseudoR pipeline to identify IS insertions in healthy human fecal  
161 metagenomes by analyzing data from three geographically disparate studies: a survey of  
162 healthy Italian adults ranging in age from 30-105 years (ITA)<sup>34</sup>, healthy individuals from a  
163 Japanese colorectal cancer study (JPN)<sup>35</sup>, and healthy rural Madagascan adults (MDG)<sup>36</sup>. Each  
164 study showed evidence of widespread IS insertion heterogeneity (Fig. 2A). Some individuals  
165 had few detectable IS insertions while others had over 100 unique IS insertions (Fig. 2B). We  
166 used relative IS depth (IS depth divided by the sum of the IS depth and the depth of reads that  
167 map to the insertion site without the insertion present) as a metric to report the abundance of IS  
168 alleles. Most insertions had a relative IS depth between 10% and 100%, demonstrating that the  
169 inserted allele exists in equilibrium with the wild type allele (Fig. 2A). We next determined the  
170 bacterial taxa that underwent extensive IS insertional activity (Fig. 2C, Fig. S2A). IS insertions  
171 were most abundant in the *Bacteroidia* and *Clostridia*. These two classes make up the majority  
172 of the healthy intestinal microbiota<sup>37</sup> and the genera *Bacteroides*, *Phocaeicola*, *Ruminococcus*,  
173 and *Blautia* accounted for the majority of IS element insertion diversity (Fig. S2A). While  
174 *Bacteroidia* IS insertions were present across all studies, the IS elements underlying these  
175 insertions varied between studies (Fig. 2D). Unique IS types for the *Bacteroidia* included  
176 ISOSDB412 (IS30 family) insertions for ITA individuals, ISOSDB18121 (IS1380 family)  
177 insertions for JPN individuals, and ISOSDB33 (IS1182 family) insertions for MDG individuals  
178 (Fig. 2D). Insertions in the *Bacteroidia* from JPN and ITA individuals were formed from shared  
179 IS elements, including ISOSDB4584 (ISL3 family), ISOSDB634 (IS982 family), and ISOSDB445  
180 (IS66 family), whereas the IS diversity in the *Bacteroidia* from MDG individuals consisted of  
181 ISOSDB250 (IS66 family), ISOSDB426 (IS630 family), and ISOSDB45 (IS256 family) insertions.

182 This suggests that regional differences contribute to IS element content or activity that drives  
183 insertion events.

184 IS insertion types among the *Clostridia* were found across all three geographic  
185 locations, with many more IS elements shared between JPN and ITA individuals (Fig. 2D).  
186 Interestingly, the *Clostridia* shared three IS family types (IS982, IS66, and IS30) with the  
187 *Bacteroidia*, yet the specific IS family members were different IS elements (Fig 2D). We  
188 conclude from this data that although the IS sequence space of these two classes of bacteria  
189 are unique, some IS families are shared and certain IS families may be more promiscuous.

190 MDG individuals, despite having similar numbers of IS insertions among their bacterial  
191 communities (Fig. 2B), had relatively low abundances of IS insertions in *Bacteroides*,  
192 *Phocaeicola*, *Blautia*, and *Bifidobacterium* and much higher abundance of IS elements  
193 associated with pathobionts including *Escherichia* and *Prevotella* (Fig. S2A)<sup>38-41</sup>. This is  
194 supported by the presence of ISOSDB45 (IS256 family) insertions that are associated with  
195 pathogenic bacteria (Fig. 2D)<sup>19,42-44</sup>.

196 IS elements can insert into coding sequences or intergenic regions of the genome which  
197 can inactivate genes or influence the expression of adjacent genes<sup>28</sup>. To measure IS insertions  
198 in intragenic versus intergenic sites, we analyzed the precise positions of all IS elements in ITA,  
199 JPN, and MDG individuals by comparing the number of intragenic insertions to intergenic  
200 insertions on a per individual basis. We found that specific IS elements had preference for  
201 intragenic or intergenic insertions (Fig. 2E). ISOSDB1159 (IS3 family), ISOSDB805 (IS3  
202 family), ISOSDB178 (ISAS1 family), and ISOSDB237 (IS4 family) preferentially inserted into  
203 intergenic loci, while ISOSDB18121 (IS1380 family), ISOSDB445 (IS66 family), and  
204 ISOSDB412 (IS30 family) inserted more frequently into intragenic loci. These data indicate that  
205 some IS elements are suited to diversify genomes through mutation whereas others may  
206 preferentially insert adjacent to coding sequences to alter gene expression.

207



208 ***IS elements frequently insert into accessory genes important for bacterial adaptation***

209 Having identified numerous IS insertions within predicted coding sequences, we  
210 analyzed open reading frames (ORFs) carrying IS insertions, termed iORFs, in the ITA, JPN,  
211 and MDG individuals. A deduplicated gene database of all predicted ORFs from the  
212 metagenomes of each study were assessed for iORF's. iORF's with insertions from a single  
213 individual were ~10-fold more abundant than iORFs with insertions from multiple individuals  
214 (Fig. 3A). This demonstrates that intestinal metagenomic IS insertions have a high degree of  
215 inter-individual variation. We next performed functional annotation of the iORF's and found five  
216 broad categories that were shared between individuals and encompassed 20.7% of iORFs (Fig.  
217 3B). Many iORFs were annotated as *susC*, *susD*, or *tonB* receptor genes in ITA and JPN  
218 individuals. These genes encode high-affinity substrate-uptake receptors for carbohydrates and  
219 cofactors<sup>45,46</sup>. *susC-D* homologs are frequently involved in the uptake of polysaccharides used  
220 for metabolism, with *Bacteroidia* species containing many different *susC-D* homologs<sup>45</sup>.  
221 Mobilome genes, including transposases, integrases, prophages, and mobile element defense  
222 genes, such as restriction modification systems, contained insertions in almost every individual  
223 across all studies. Exopolysaccharide biogenesis genes, such as LPS modifying enzymes and  
224 cell wall synthesis glycosyltransferases, were consistent IS element insertion targets. Cell wall  
225 and membrane modifications are crucial for *in vivo* survival by avoiding host immunity and  
226 during competition with other bacteria<sup>47</sup>. Finally, antibiotic resistance genes frequently contained  
227 IS insertions, including the genes *tetQ* and *ermF* in JPN and ITA individuals. IS insertions were  
228 enriched in all functional categories except the EPS biogenesis genes, when comparing the  
229 abundance of iORFs with all predicted protein coding sequences (Fig. 3C, Fig. S2B). Together,  
230 these data show that genes involved in accessory metabolic functions, antibiotic resistance, and  
231 genomic plasticity are common IS insertion targets.

232 We next asked if certain iORFs were shared between individuals from the three studies.  
233 Although infrequent, a few iORFs were shared. 14% and 37% of ITA and JPN individuals,

234 respectively, had IS insertions in the gene *ermF*, a macrolide resistance gene, and 3.2% and  
235 9.8% of ITA and JPN individuals, respectively, had IS insertions in *KAP*, a P-loop NTPase  
236 predicted to be involved in phage defense (Fig. 3D)<sup>48,49</sup>. 7.9% and 6.1% of ITA and MDG  
237 individuals, respectively, shared IS insertions in *shufflon*, a gene encoding an invertase that  
238 regulates pilin phase variation (Fig. 3D)<sup>50</sup>. We found that iORF functional classes were  
239 conserved across diverse intestinal bacteria (Fig. 3E) yet the IS types responsible for these  
240 insertions differed among the various classes of bacteria (Fig. 3F). This demonstrates that  
241 although IS elements target similar genes within disparate bacteria, the types of IS elements  
242 that promote these diversification events are specific to certain classes of bacteria.

243 Multiple iORF's were classified as transposases (Fig. 3B) and examples of IS elements  
244 inserting in other transposase genes has been previously reported<sup>51</sup>. In order to understand the  
245 dynamics of IS insertions in other IS elements, we classified both the transposase iORF and the  
246 IS forming the insertion by IS family (Fig. 3G). We found multiple examples of both self-targeting  
247 (an IS inserting into a closely-related IS) and orthologous-targeting (an IS element inserting into  
248 an unrelated IS). We found that IS families such as ISL3, IS4, IS110, and IS256 experienced  
249 promiscuous insertion events. These results suggest that IS self- and orthologous-targeting  
250 could be a mechanism to control IS mobilization of genetic traits.

251

### 252 ***IS elements provide mutational diversity to Bacteroides species***

253 Genome wide mutagenesis of *Bacteroides thetaiotaomicron* (*Bt*) identified genes that  
254 support adaptation to environmental pressures, including antibiotics, bile acids, and carbon  
255 sources<sup>52</sup>. We used this dataset to evaluate whether we could identify similar fitness  
256 determinants as iORFs within intestinal *Bacteroides*. We searched our iORF database for  
257 homologs to these fitness-associated ORFs from *Bt* and found multiple closely related iORFs  
258 that likely influence *Bacteroides* fitness both positively and negatively (Fig. S3A). Examples  
259 include iORFs that provide fitness advantages during growth in the presence of the antibiotics,

260 such as doxycycline, and during hyaluronic acid and glucosamine consumption (Fig. S3A).  
261 Interestingly, we found iORFs associated with bacterial fitness during exposure to the  
262 antipsychotic medication chlorpromazine (Fig S3A) which is associated with compositional  
263 changes and antibiotic resistance of the microbiota<sup>53-56</sup>. Additionally, we found multiple IS  
264 insertions in homologs of the *Bt susC* gene BT1119 (Fig. S3B). Inactivation of BT1119  
265 decreases fitness during growth on galacturonic acid<sup>52</sup>.

266 Our *in silico* analysis shows that the intestinal *Bacteroidia* experience large-scale IS  
267 mobilization into discrete groups of genes involved in carbohydrate utilization,  
268 exopolysaccharide synthesis, and mobile genetic element interactions. To test if the activation  
269 of an IS element leads to insertion into these classes of genes, we focused on ISOSDB412  
270 (IS30 family member IS4351), an IS element is that is native to strains of *Bt* and *Bacteroides*  
271 *fragilis* (*Bf*)<sup>57</sup>. We transformed a low-copy number plasmid carrying an *ermF* cassette disrupted  
272 by ISOSDB412 into *Bt* VPI-5482 and *Bf* NCTC 9343. These strains lack native copies of  
273 ISOSDB412 which allowed us to study this IS element in the context of a genetic arrangement  
274 that we found from our analysis of the microbiota. Following growth, we isolated their genomic  
275 DNA and performed IS-Seq which enriches for ISOSDB412 amplicons to identify their insertion  
276 locations<sup>19</sup>. Both *Bt* and *Bf* strains carrying the ISOSDB412 plasmid obtained numerous  
277 ISOSDB412 insertions throughout their genomes compared to controls that lacked the  
278 ISOSDB412 plasmid construct (Fig. 4A, Fig. 4D). As predicted, ISOSDB412 insertions were  
279 enriched in gene categories reflected from our findings from insertions from the human  
280 microbiota (Fig. 4B, Fig. 4E). In *Bt*, ISOSDB412 insertions were enriched in *susC-D/tonB* and  
281 EPS biogenesis genes, whereas *Bf* acquired an abundance of insertions in *susC-D/tonB* genes  
282 despite a significantly lower number of ISOSDB412 insertion events compared to *Bt* (Fig. S4A).  
283 Additionally, insertions were more frequently found in intragenic loci compared to intergenic loci,  
284 confirming our findings from the intestinal microbiota (Fig. 4C, Fig. 4F). These results  
285 demonstrate that IS elements can rapidly diversify *Bacteroidia* genomes.

286 Our discovery that IS insertions target accessory genes suggests that these IS insertions  
287 inactivate genes that are currently dispensable for intestinal survival. To explore this, we  
288 measured IS insertional dynamics in a nutrient-deplete environment with glucose as the sole  
289 carbon source. We hypothesized that a lack of fiber and complex carbon sources, high levels of  
290 glucose, and single sources of iron and nitrogen, would incentivize higher rates of IS insertions  
291 to inactivate costly metabolic machinery needed for competition in complex nutritional  
292 environments. We measured ISOSDB412 insertions from three *Bt* colonies after three  
293 sequential passages in either complex media (BHIS) or minimal media (MM) (Fig. 4G, Fig. 4H,  
294 Fig. 4I). We found that colonies passaged in MM had substantially more ISOSDB412 insertions  
295 compared to BHIS-passaged colonies. Numerous insertions were found in the open reading  
296 frame BT3642, a Na<sup>+</sup>-dependent transporter (Fig. S4B) in MM colonies, but not in BHIS  
297 colonies. This gene has been shown to be detrimental for growth in glucose minimal media<sup>52</sup>.

298 Next, we measured ISOSDB412 abundance in *Bt* cells chronically infected with the  
299 *Crassvirales* DAC15 or DAC17 (Fig. 4J, 4K, 4L). *Crassvirales* are bacteriophages that infect  
300 *Bacteroides* species and are abundant in the human intestine<sup>58</sup>. *Bt* cells become chronically  
301 infected by these phages and shed them during growth (Fig. S4C). While DAC15 and DAC17  
302 share 99.24% nucleotide identity over 98% of their genomes, DAC17 infection is associated  
303 with an increased IS insertions genome-wide (Fig. 4J, Fig. 4K) which inserted into genes  
304 involved in EPS biogenesis (Fig. 4L). Furthermore, almost all of the infected strains carried IS  
305 insertions in the CPS3 locus (Fig. S4D), which is crucial for productive phage infection and likely  
306 leads to phage resistance<sup>59</sup>. Together, these results show that IS diversification of the *Bt*  
307 genome is more prevalent under nutrient-limited conditions and during infection with intestinal-  
308 resident phages. This indicates that IS activity supports *Bt* adaptation when faced with fitness  
309 constraints.

310

311 ***Temporal monitoring of IS activity shows that IS insertions are maintained over time.***

312 IS insertions were found in specific genetic loci coexisting with the wild type allele  
313 lacking the IS insertion, indicating that both versions of the allele are maintained in equilibrium.  
314 Previous work has shown that many phyla of intestinal bacteria harbor variable numbers of IS  
315 insertions<sup>60</sup>. To understand the temporal longevity of IS insertions in the microbiota, we  
316 analyzed longitudinal fecal metagenomic samples from healthy individuals<sup>61,62</sup>. Using a set of  
317 two individuals whose fecal samples were collected over the course of 76 and 91 weeks<sup>61</sup>, we  
318 measured the IS landscape of their microbiotas using pseudoR. We also analyzed longitudinal  
319 samples from an additional 10 individuals from a separate study<sup>62</sup>. A representative individual's  
320 IS dynamics are in Fig. 5A-B. We used the assemblies from the first timepoint (indicated as  
321 week 0 in Fig. 5A) as the reference for the pseudoR pipeline which was then compared to all  
322 other time points to assess the maintenance of ancestral IS insertions and acquisition of new IS  
323 insertions. We found that many IS insertions are maintained for the entire time course and that  
324 some of these insertions frequently went in and out of detection (Fig. 5A). New insertions not  
325 present at week 0 arose at almost every timepoint, with a variable number of insertions per  
326 timepoint. New insertions were maintained for extended periods of time while others were only  
327 detected at the initial timepoint. These results demonstrate that IS elements are stably carried in  
328 the microbiota and are actively forming new insertions, similar to the accumulation of mutations  
329 in laboratory-evolved strains<sup>63-65</sup>.

330 Next, we analyzed whether host bacterial abundance accounts for the detection of new  
331 IS elements in all individuals (Fig. S5A). Increasing levels of host bacterial IS elements could  
332 generate higher sequencing read depth and more detection power for new IS insertions. For  
333 every insertion not present at week 0, we compared the insertion site's read depth (a marker of  
334 host abundance) to the maximum insertion site depth of all earlier timepoints (prior to the  
335 detection of the insertion). Insertions with depths equal to or less than 200% of the previous  
336 maximum insertion site depth were considered to arise from new insertional activity (Fig. S5B).

337 We found that the majority of new insertions could be accounted for as active IS insertions  
338 independent of bacterial abundance (Fig. S5C).

339         Insertions across the time series included diverse IS families and were frequently  
340 associated with the *Clostridia* and *Bacilli* (Fig. 5B). Additionally, we observed that the rate of  
341 new insertions per week for every individual ranged on average from around 1 to 10 new  
342 insertions. This value was calculated by dividing the number of new insertions per timepoint by  
343 the number of weeks between the current timepoint and the previous timepoint. We assumed a  
344 constant rate of transposition as has been used in previous studies<sup>63,64</sup>. Intra- and inter-personal  
345 variation in this rate could be due to both variations in selective pressure in the microbiota and  
346 technical variation, such as altered sequencing depth and library diversity. We also found that  
347 the maintenance, loss, and gain of IS elements tracked with common bacterial accessory genes  
348 that we established to be “hot spots” for IS insertions (Fig. 5C, Fig. 5D).

349

### 350 ***IS elements are efficiently transferred and maintained within new individuals***

351         Having discovered that individual microbiotas have unique patterns of IS insertions, we  
352 wanted to understand how the human host influences the dynamics of IS insertions within the  
353 microbiota. To test this, we used pseudoR to profile the IS insertions during fecal microbiota  
354 transplantation (FMT) where the microbiotas of FMT donors and recipients were longitudinally  
355 sampled before and after fecal transplantation<sup>61</sup>. We compared the IS insertional landscape in  
356 both the donors and recipients using the assembly of the donor’s transplanted microbiota as a  
357 reference. A representative recipient and donor’s IS dynamics are shown in Fig. 6A. Donor-  
358 derived communities harbored IS insertions that were stably maintained over one year in the  
359 FMT recipients (Fig. 6A). Insertions present prior to transplantation in recipients were lost, but a  
360 minority returned at later timepoints. Recipients maintained significantly less IS insertions that  
361 were present at week 0 compared to the donors (Fig. 6C), but both donor and recipients had  
362 similar rates of new insertions (Fig. 6D). To understand if IS insertional activity was similar

363 between host and recipient, we compared the pattern of new shared insertions in donors and  
364 recipients at all timepoints post transplantation (Fig. 6B & Fig. S6). We found multiple instances  
365 of the same newly detected insertion arising in both donor and recipients at the same timepoint.  
366 These results demonstrate that IS insertions can be stably maintained in new hosts for  
367 extended periods of time and that new IS mobilization occurs at similar rates and patterns in  
368 new hosts.

369

### 370 ***Antibiotics drive widespread loss of IS insertions within the microbiota***

371 Considering IS insertions were found to persist for prolonged periods of time within the  
372 microbiota and were portable between individuals, we wanted to know what would happen to IS  
373 diversity if a stable community was disrupted. To test this, we analyzed the IS composition  
374 before, during, and after broad spectrum antibiotic treatment<sup>66</sup>. The metagenome of the  
375 microbiota preceding antibiotic treatment was used as the reference for IS comparison using  
376 pseudoR. As expected, antibiotic treatment caused a substantial loss of IS diversity, which was  
377 not fully restored after treatment (Fig. 7A). The starkest example was sample ERAS10.  
378 Extensive IS diversity was present at week 0 in ERAS10 before antibiotic treatment and by at  
379 week 0.6 there were no detectable IS signatures nor did any of the original ISs return by week  
380 26 post antibiotic therapy. To summarize these findings, we compared the rate of maintenance  
381 of pre-antibiotic treatment insertions in individuals treated with antibiotics and those who were  
382 not. Antibiotic treatment was associated with a significant decrease in the ability of the  
383 microbiota to maintain IS insertions (Fig. 7D).

384

### 385 ***IS insertion into *susC-D/tonB* loci is associated with diet intervention.***

386 Our analysis had identified *susC-D/tonB* genes as major targets for IS insertions,  
387 suggesting that ISs can modulate carbohydrate metabolism in the *Bacteroidia* (Fig. 3), and we  
388 showed in *Bt* that nutrient stress promotes insertions into predictable metabolic loci (Fig. 4).



389 Based on this data, we suspected that a radical diet intervention in humans would lead to a shift  
390 in IS insertions in metabolic-associated genes such as *susC-D/tonB* loci. To test this hypothesis,  
391 we analyzed the IS insertions in the intestinal microbiota of obese individuals before, during,  
392 and after a year-long diet intervention<sup>67</sup>. Participants in this study received a low-calorie formula-  
393 based diet for 12 weeks, followed by a 6-week period of phasing out the formula diet for solid  
394 food without changing total caloric intake, followed by a 7-week phase where caloric intake was  
395 increased while preventing weight gain<sup>68</sup>. We found that ancestral *susC-D/tonB* insertions were  
396 frequently lost during the course of the diet study and new insertions in *susC-D/tonB* genes  
397 arose after the diet intervention ended (Fig. 7C). Additionally, insertions arose in the *susC*-  
398 *D/tonB* homolog BT1119 (Fig. 7D). Together, these results demonstrate that diet alteration is  
399 associated with perturbations in IS insertions in *susC-D/tonB* genes.

400

## 401 Discussion

402 IS elements are fundamental to the evolution of bacterial genomes. Despite this, IS  
403 diversity and function within polymicrobial communities is understudied. Here, we built a  
404 computational pipeline for identifying IS insertions within complex metagenomic DNA  
405 sequences. This pipeline, which we call pseudoR, relies on an open-source IS element  
406 database (ISOSDB), which vastly improves nucleotide diversity compared to current state-of-  
407 the-art databases. Using pseudoR, we found that IS elements contribute to high levels of  
408 bacterial genomic diversification within the microbiota, are maintained at specific loci for  
409 extended periods of time, can be efficiently transferred between individuals, and experience  
410 fluctuations within bacterial populations following perturbation. Together, these results  
411 demonstrate that IS elements are important genetic elements that can dictate genotype diversity  
412 within the microbiota.

413 Using previously published metagenomic datasets, we show that the majority of open  
414 reading frames containing IS insertions (iORFs) are unique and not shared between individuals.



415 This is similar to the observation that polymorphism diversity in the human intestinal microbiota  
416 is more likely to be unique than shared<sup>69</sup>. Our work expands on this idea and suggests that IS  
417 activity is a part of each person's "fingerprint" of microbial diversity.

418 iORFs were frequently annotated within five broad categories: *susC-D/tonB*, mobilome  
419 genes, EPS genes, antibiotic resistance genes, and MGE resistance genes. Genes belonging to  
420 these categories are considered accessory genes and are often non-essential. Interestingly,  
421 genes regulated by DNA inversions, including phase variation, fall into similar functional  
422 categories as those targeted by IS insertions<sup>70,71</sup>. This suggests that insertions and inversions  
423 control gene expression of the microbiota to position bacteria for optimal adaptation.

424 Additionally, *susC-D/tonB* receptors are often targets of nucleotide evolution in the human  
425 intestine, possibly to help gain new abilities based on substrate availability<sup>21</sup>. In support of this, a  
426 SusC epitope activates T cells to promote an anti-inflammatory IL-10 response in healthy  
427 individuals and induces a pro-inflammatory IL-17A response in people with Crohn's disease<sup>72</sup>.  
428 This suggests that IS elements influence the immunomodulatory capacity of the microbiota.

429 The microbiome of urban individuals is less-well suited to degrade diverse  
430 polysaccharides compared to rural individuals<sup>73</sup>. Here, we found that urban individuals (those in  
431 the ITA and JPN cohorts) have extensive modulation of the microbiota with high rates of IS  
432 insertions in *susC-D/tonB* genes, compared to individuals living in rural settings (MDG cohort).  
433 This could partly be explained by in ITA and JPN individuals as they have a dominance of IS  
434 insertions in *Bacteroides* and *Phocaeicola* bacterial species, while MDG individuals have limited  
435 *Bacteroidia* IS insertions. However, we expect that the varied diet of MDG individuals, which  
436 includes wild meat and plants<sup>74</sup>, partially selects for a more diverse set of functional *susC*-  
437 *D/tonB* receptors compared to individuals consuming an industrialized diet. Further work to  
438 characterize IS insertions in individuals with rural lifestyles, such as the Hadza hunter  
439 gatherers<sup>75</sup>, will better demonstrate how IS elements impact nutrient acquisition.

440 iORFs were common among MGE resistance and macrolide resistance (*ermF*) genes<sup>76</sup>.  
441 Both of these classes of genes have been reported to be targets of IS inactivation<sup>19,33</sup>. Since  
442 these are heterogenous populations that co-exist between genes carrying or lacking IS  
443 insertions, we hypothesize that IS insertions in these genes maintains a low level of population-  
444 wide MGE and antibiotic resistance and reduces the burden of expressing the resistance gene.  
445 Such a “hedge-betting” strategy would be advantageous upon antibiotic or phage exposure  
446 where the population can regain resistance thorough selection of variants.

447 Prior to this study, it was unknown how stable IS elements were in bacterial genomes  
448 within host associated microbiotas. We found that specific IS insertions were detectable for just  
449 under two years, demonstrating that IS insertions within specific genetic loci are often not  
450 sanitized from the population. These findings are analogous to the discovery of nucleotide  
451 polymorphism conservation within the microbiota<sup>77</sup>. Additionally, we established that IS  
452 elements can be stably transferred between individuals. Donor-derived bacterial communities  
453 have been shown to persist in recipients following FMT<sup>78-80</sup>. We conclude that IS insertions are  
454 stable in host associated microbiotas and may impart a minimal fitness cost to their bacterial  
455 host.

456 Bacterial diversity frequently rebounds after antibiotic treatment<sup>66,81</sup>, but how bacterial  
457 communities assemble at the strain level is more varied and includes widespread loss of  
458 mutations and enrichment of others<sup>82</sup>. We found that IS insertions were readily lost after  
459 antibiotic treatment. Our results suggest that ISs can be viewed as strain-level features that are  
460 more variable than taxonomic-level diversity following perturbation.

461 In summary, the development of a contemporary and stringently curated IS database,  
462 combined with a streamlined computational approach to identify IS elements from metagenomic  
463 data, has revealed insights into how IS elements shape the genomes of the microbiota and sets  
464 the stage for exploring how specific IS variants in the microbiota influence human health.  
465 However, a few limitations to the tools and study exist. First, delineation of IS insertion sites

466 between closely related strains is imperfect, thus insertions between very closely related strains  
467 may group together and fail to resolve. Work from the intestinal microbiota has found that most  
468 species are represented by one dominant strain and that these strains are stable over long  
469 periods<sup>83</sup>, suggesting that the insertion sites that we measured are from subpopulations  
470 originating from single strains. Second, we do not understand how IS insertions influence the  
471 fitness of the microbiota. We can begin to overcome this problem by assembling and assessing  
472 Tn-Seq libraries of diverse intestinal bacteria under conditions relevant to the intestine and in  
473 animal colonization experiments. Coupling such studies with pseudoR analyses of microbiota  
474 datasets would begin to help determine what IS insertion sites are beneficial or detrimental to  
475 commensal bacteria. Third, the pseudoR pipeline relies on assemblies containing some level of  
476 the wild type allele for comparison to an IS insertion at that same allele. This limits the detection  
477 of IS elements that assemble as part of the reference contig. Conceivably, an inverse method to  
478 find wild type alleles in IS-allele assemblies can be built and be implemented into a future  
479 release of pseudoR. Fourth, the single reference mode of pseudoR excludes assemblies from  
480 later timepoints to prevent over-assembly and focuses the analysis on the initial timepoint. This  
481 hinders our understanding of how IS elements are impacting the microbiota not present at the  
482 initial timepoints.

483

## 484 **Materials and Methods**

### 485 **Data and Code Availability**

486 IS-Seq data have been deposited at NCBI SRA and are publicly available as of the date  
487 of publication. Accession numbers are listed in the Key Resources Table. This paper analyzes  
488 existing, publicly available data. The accession numbers for these datasets are listed in the Key  
489 Resources Table. All original code has been deposited at GitHub and is publicly available as of  
490 the date of publication. DOIs are listed in the Key Resources Table.

491

## 492 **Experimental Model and Study Participant Details**

493 *Bacteroides thetaiotaomicron* VPI-5482, *Bacteroides thetaiotaomicron* VPI-5482 CPS3,  
494 and *Bacteroides fragilis* NCTC 9343 were cultured as previously described<sup>84,85</sup>. Briefly, these  
495 strains were grown in brain-heart infusion (BHI) broth (Becton Dickinson, Franklin Lakes, NJ)  
496 supplemented with 1 g/L cysteine, 5% w/v NaHCO<sub>3</sub>, and 5 mg/L hemin (BHIS), Varel-Bryant  
497 minimal media<sup>86</sup> supplemented with 28 mM glucose, or *Bacteroides* phage recovery medium  
498 (BPRM)<sup>87</sup> at 37° C in a Coy Type A vinyl anaerobic chamber in an atmosphere of 5% hydrogen,  
499 20% carbon dioxide, and balanced nitrogen (Coy Lab Products, Grass Lake, MI). For growth on  
500 solid-media we used BHI agar supplemented with 10% defibrinated calf blood (Colorado Serum  
501 Company, Denver, CO). *Escherichia coli* S17-1 was grown in Lennox L broth (Fisher Scientific,  
502 Hampton, NH) with aeration at 37° C. Tetracycline was used at 2 µg/mL, gentamicin was used  
503 at 200 µg/mL, and ampicillin was used at 100 µg/mL.

504

## 505 **Quantification and Statistical Analysis**

506 Details of statistical analyses for specific figures can be found in the figure legends. All  
507 statistical analyses were performed using Graphpad Prism, with the exception of Fisher's exact  
508 test which was performed using R.

509

## 510 **Creation of the ISOSDB**

511 All genomes classified as "complete" in NCBI Assembly were downloaded on  
512 05/08/2023 using bit v1.8.57<sup>88</sup>. IS elements were identified using OASIS<sup>27</sup>. This program uses  
513 annotated transposases as points for sequence extension and comparison to find complete IS

514 elements. Identified IS elements were filtered using the following criteria: 1) multiple (minimum  
515 of 2) complete copies of the element must be present in at least one genome and 2) the  
516 elements must contain identified inverted repeat sequences. To supplement these genomes, we  
517 identified IS elements in hybrid-assembled MAGs from a large human intestinal microbiota  
518 study<sup>26</sup>. These metagenomes were annotated with Prokka v1.14.6<sup>89</sup>, processed as described  
519 above, and then combined with the IS elements identified from the genomes from NCBI  
520 Assembly. Redundant IS elements in the final database were deduplicated using CD-HIT-EST<sup>90</sup>  
521 with a 95% sequence cutoff and a word length of 9. IS element homologs in ISFinder were  
522 found using either blastn (complete elements) with a minimum e-value of 0.000001 and a  
523 minimum length of alignment of 224 bp or blastp (transposases) with a minimum e-value of  
524 0.000001<sup>91</sup>. To further confirm that IS elements in the ISOSDB are legitimate, the transposases  
525 of IS elements that lacked nucleotide homology to IS elements in ISFinder were profiled using  
526 InterProScan<sup>92</sup> and NCBI Conserved Domain Database<sup>93</sup> using default settings. Putative  
527 transposases that lacked domains associated with transposases (such as “DDE superfamily  
528 endonuclease”, “Integrase core domain”, and “Transposase”) were removed from the final  
529 ISOSDB. The ISOSDB and pseudoR pipeline is freely available at  
530 <https://github.com/joshuakirsch/pseudoR>. Each IS element in this database is given a unique  
531 numeric identifier. Clustering at the amino acid and nucleotide level was performed using  
532 MMSeqs2 v15.6f452<sup>94</sup> with coverage mode 0 and a minimum coverage of 80%.

533

### 534 **pseudoR pipeline**

535 To characterize IS elements and their insertion sites in metagenomic DNA sequences  
536 we built the pseudoR pipeline. This tool relies on deeply-sequenced short read Illumina data  
537 and can be used for both metagenomic and single isolate genome data.

538 For this study, reads were downloaded from NCBI SRA <sup>95</sup> using fasterq-dump v2.11.0  
539 from these studies <sup>34-36,61,66,67</sup>. Study accession numbers are provided in the Key Resources  
540 Table. Duplication removal, quality trimming, and read decontamination was performed using  
541 programs from the BBTools software suite <sup>96</sup>. PCR duplicated reads were removed with  
542 clumpify.sh with the flag “subs=0”. Adapter and quality trimming was performed with bbduk.sh  
543 and human, mouse, and phi29 read contamination was removed using bbsplit.sh. Cleaned and  
544 deduplicated reads were assembled using MEGAHIT v1.2.7 with the “meta-large” preset (-k-  
545 max 127 -k-min 27 -k-step 10) <sup>97</sup>. All contigs used in downstream analyses were greater than 1  
546 kB.

547 We built two modes for IS identification: single and multi mode. Single mode is used to  
548 identify IS insertions within the microbiota from longitudinal samples from the same individual. In  
549 this mode, only the individual’s starting timepoint assembly is used to find IS insertions. This  
550 approach reduces the chance that meaningful information is lost during clustering of multiple  
551 assemblies from multiple timepoints. The single reference mode can be used for evolution  
552 studies where a single population is compared between different treatments. Multi mode is used  
553 for comparing the insertional patterns between multiple individuals. When using the multi  
554 reference mode, reads are first mapped against the sample’s own assembly and then remapped  
555 against a combined and deduplicated ORF database built from every sample’s assembly.

556 Before the pipeline was initially run, a database of IS termini was built by merging the  
557 first and last 150 bp of each IS in the ISOSDB together and deduplicating these merged  
558 sequences using CD-HIT-EST <sup>90</sup> with a minimum sequence identity of 90%. The merged  
559 sequences were split into 150 bp sequences and a blastn database <sup>91</sup> was built from this  
560 deduplicated dataset.

561 At the beginning of the pipeline, ORFs in assemblies are predicted using prodigal.py (a  
562 parallelizable wrapper of prodigal <sup>98</sup>) and deduplicated using dedupe.sh. Reads are aligned first

563 to the reference assembly using Bowtie2<sup>99</sup>. Any mapped read, including discordantly mapped  
564 reads, are considered positive hits. Unmapped reads are collected and aligned to the IS termini  
565 database using blastn and then filtered using a custom R script. This filtering script ensures that  
566 the IS termini is properly positioned on the read such that the remainder of the read is outside of  
567 the IS element. The IS termini are removed and the trimmed reads are re-mapped to the  
568 sample's assembly as unpaired reads using Bowtie2. Following this, the original mapped reads  
569 and IS-termini trimmed reads are re-mapped against the deduplicated gene database in  
570 nucleotide format.

571       Following read mapping completion in both single and multi mode, a custom R script is  
572 used to identify DNA insertion sites with read mapping from both the left and right terminus of  
573 the IS element at most 20 bp away from one another and this script compiles read abundances  
574 for these regions. Mosdepth v0.3.3<sup>100</sup> is used to determine the sequencing depth of the  
575 uninserted allele for the loci described above. Seqkit v2.2.0<sup>101</sup>, samtools v1.6<sup>102</sup>, R, ggplot2,  
576 tidy, and MetBrewer are used for various computational tasks. Scripts to reproduce all data  
577 analysis presented here are available in the GitHub repository.

578

#### 579 **iORFs assoated with *B. thetaiotaomicron***

580       *B. thetaiotaomicron* VPI-5482 coding sequences were downloaded from  
581 fit.genomics.lbl.gov. Homologs to iORFs were found using blastp with a maximum e-value of  
582 0.00005 and a minimum identity of 75%. Hits to multiple related fitness determinants were  
583 filtered to include the representative with the strongest fitness value.

584

#### 585 *Functional and taxonomic classification of contigs and ORFs*

586       Metagenomic sequences with IS insertions were functionally annotated using eggNOG  
587 mapper v2<sup>103</sup>. Orthologous groups were cross-validated using the COG database<sup>104</sup>. ORFs were

588 classified as *susCD/tonB* if they contained a PFAM which contained the phrases “SusC”,  
589 “SusD”, or “tonB”. Anti-MGE ORFs were classified as such if they classified as COG5340,  
590 COG2189, COG0286, COG0732, COG0827, or COG4217. Exopolysaccharide biogenesis  
591 ORFs and mobile element ORFs were classified as belonging to COG category “M” or ‘X”,  
592 respectively. Antibiotic resistance genes were identified using CARD RGI 6.0.0<sup>105</sup>. ORFs and  
593 contigs containing IS insertions were classified using Kraken2 v2.0.7<sup>106</sup>.

594

## 595 **Bacteria**

596 *Bacteroides thetaiotaomicron* VPI-5482, *Bacteroides thetaiotaomicron* VPI-5482 CPS3<sup>85</sup>,  
597 and *Bacteroides fragilis* NCTC 9343 were cultured as previously described<sup>84</sup>. Briefly, these  
598 strains were grown in brain-heart infusion (BHI) broth (Becton Dickinson, Franklin Lakes, NJ)  
599 supplemented with 1 g/L cysteine, 5% w/v NaHCO<sub>3</sub>, and 5 mg/L hemin (BHIS), Varel-Bryant  
600 minimal media<sup>86</sup> supplemented with 28 mM glucose, or *Bacteroides* phage recovery medium  
601 (BPRM)<sup>87</sup> at 37° C in a Coy Type A vinyl anaerobic chamber in an atmosphere of 5% hydrogen,  
602 20% carbon dioxide, and balanced nitrogen (Coy Lab Products, Grass Lake, MI). For growth on  
603 solid-media we used BHI agar supplemented with 10% defibrinated calf blood (Colorado Serum  
604 Company, Denver, CO). *Escherichia coli* S17-1 was grown in Lennox L broth (Fisher Scientific,  
605 Hampton, NH) with aeration at 37° C. Tetracycline was used at 2 µg/mL, gentamicin was used  
606 at 200 µg/mL, and ampicillin was used at 100 µg/mL.

607

## 608 **DNA extraction and IS-Seq**

609 Genomic DNA was extracted from 1.5 mL cultures of *Bacteroides* strains using the  
610 Zymobionics DNA Miniprep kit (Zymo Research, Irvine, CA) and used as input for IS-Seq as  
611 described previously<sup>19</sup>. Briefly, NGS libraries were produced using the Illumina DNA Prep Kit  
612 (Illumina, San Diego, CA) and amplified using ISOSDB412 IS-Seq Step1 and p7 primers for 13



613 cycles using Q5 Master Mix (New England Biolabs, Ipswich, MA). The products of this reaction  
614 were amplified with IS-Seq Step2 and p7 primers for 9 cycles using Q5 Master Mix and  
615 sequenced on a Novaseq 6000 at Novogene (Sacramento, CA). R1 reads were binned and  
616 trimmed of the ISOSDB412 terminus and adapters using cutadapt v1.1.18<sup>107</sup>. To remove PCR  
617 duplicates, R2 pairs of R1 reads that contained the ISOSDB412 terminus were binned and  
618 deduplicated using dedupe.sh from the BBTools suite with the flag minidentity=100.  
619 Deduplication of R2 reads ensures that each amplified read pair is a unique molecule, while  
620 maintaining read depth information of the R1 (IS-amplified) read. This set of deduplicated R2  
621 reads was re-paired to trimmed R1 reads with reformat.sh from the BBTools suite and these  
622 pairs were aligned to the host genome using Bowtie2. R1 read depth at each genomic position  
623 was calculated using bedtools v2.30.0<sup>108</sup> IS-seq reads can be found at the European  
624 Nucleotide Archive under study accession number PRJEB66483.

625

## 626 **DNA manipulation and cloning**

627 Primers and plasmids used in this study are listed in the Key Resources Table. All  
628 plasmid constructs were made using Gibson assembly master mix (New England Biolabs,  
629 Ipswich, MA). Assembled constructs were electroporated into electrocompetent *E. coli* S17-1.  
630 These cells were prepared by washing cell pellets three times in ice-cold electroporation buffer  
631 (0.5 M sucrose, 10% glycerol). The resulting transformants were mated with *B. thetaiotaomicron*  
632 or *B. fragilis* by mixing 500  $\mu$ L of stationary phase *E. coli* S17-1 and 500  $\mu$ L of stationary phase  
633 *Bacteroides* on BHI blood agar overnight at 37° C under aerobic conditions. Transconjugants  
634 were selected by scraping the bacterial lawns into BHI and plating serial dilutions on BHI blood  
635 agar supplemented with tetracycline and gentamicin, and incubating at 37°C anaerobically for  
636 48 hours. The ISOSDB412 (IS4351) DNA sequence construct was purchased from Twist  
637 Biosciences (San Francisco, CA). pB006 (Addgene plasmid #182320), a gift from Dr. Lei Dai,

638 was used as a shuttle vector and purchased from Addgene (Watertown, MA)<sup>109</sup>. The *tetM*  
639 cassette was cloned from pCIE-*tetM*<sup>110</sup> and the *ermF* cassette was cloned from pG10K, a gift  
640 from Dr. Janina Lewis (Addgene plasmid #191377) and purchased from Addgene<sup>111</sup>.

641

#### 642 ***B. thetaiotaomicron* passaging experiment**

643 *B. thetaiotaomicron* was grown overnight in BHIS and then subcultured 1:100 into either  
644 Varel-Bryant minimal media or BHIS containing antibiotic and grown overnight. The next day,  
645 bacteria cultured in BHIS were subcultured 1:100 into BHIS and bacteria cultured in Varel-  
646 Bryant minimal media cultured were subcultured 1:100 into Varel-Bryant minimal media with  
647 antibiotic. After overnight growth, this passaging was repeated once more. Genomic DNA was  
648 isolated and the final passage was sequenced as described above.

649

#### 650 ***B. thetaiotaomicron* phage infection**

651 *B. thetaiotamicron* CPS3 (a mutant of *B. thetaiotamicron* VPI-5482 expressing only the  
652 CPS3 capsule)<sup>85</sup> was transformed with pB6T-ermF-IS4351 and grown overnight in *Bacteroides*  
653 phage recovery medium (BPRM) with antibiotic. Overnight cultures were diluted to OD<sub>600</sub> of 1.0  
654 in phage buffer<sup>59</sup> and was plated on BPRM agar containing tetracycline and 1x10<sup>8</sup> PFU/mL of  
655 either DAC15 or DAC17. Dilutions of resuspended overnight culture were also plated on BPRM  
656 containing tetracycline. Plated cultures on DAC15 agar media were incubated at 37° C for 48  
657 hours and individual colonies were picked and patched onto fresh BPRM plates with DAC15.  
658 This process was repeated. Cultures plated on DAC17 agar and agar without phage were  
659 similarly passaged. Passaged colonies were cultured into BPRM broth without phage and  
660 incubated for 48 hours at 37° C. Genomic DNA was isolated and sequenced as described  
661 above.

662

#### 663 **Enumeration of infectious phage particles**

664 90  $\mu$ L of supernatant from liquid cultures of passaged colonies were mixed with 10  $\mu$ L  
665 chloroform (Fisher Scientific), centrifuged for 1 minute at 21,000 RCF at 25° C, and the  
666 supernatant was collected. Dilutions of this supernatant were made in phage buffer and 5  $\mu$ L  
667 spots of the dilutions were plated on a BPRM plate containing *B. thetaiotamicron* CPS3  
668 embedded in 0.35% BPRM top agar, and incubated at 37° C overnight.

669

## 670 **Acknowledgements**

671 We would like to thank the members of the Duerkop lab, Dr. A. Murat Eren, and Dr. Alejandro  
672 Reyes Muñoz for providing useful insights related to this project. This work was supported by  
673 the National Institutes of Health grants R01AI141479 (B.A.D.), T32AI052066 (J.M.K),  
674 F31AI169976 (J.M.K.), and R35GM150996 (A.J.H). The funders had no role in the study design,  
675 data collection and analysis, decision to publish, or preparation of the manuscript.

676

## 677 **Author Contributions**

678 Conceptualization, J.M.K., B.A.D.; Methodology, J.M.K., B.A.D.; Software, J.M.K.; Validation,  
679 J.M.K.; Formal Analysis, J.M.K.; Investigation, J.M.K.; Resources, B.A.D., A.J.H.; Data Curation,  
680 J.M.K.; Writing – Original Draft, J.M.K., A.J.H., B.A.D.; Writing – Review & Editing, J.M.K.,  
681 B.A.D.; Visualization, J.M.K., B.A.D.; Supervision, B.A.D.; Project Administration, B.A.D.;  
682 Funding Acquisition, J.M.K., A.J.H., B.A.D.

683

## 684 **Declaration of Interests**

685 B.A.D. is a co-founder and shareholder of Ancilia Biosciences.

686

## 687 **Figure Legends**

688 **Figure 1. The ISOSDB: a database of diverse and complete ISs.** (A) Number of unique IS  
689 sequences in ISFinder and the ISOSDB. (B) Comparison of transposase (Tnp amino acid) and

690 nucleotide sequences of the full ISs from the ISOSDB to the ISs from ISFinder. (C) Numbers of  
691 clusters of ORFs and full nucleotide sequences in the ISOSDB for a range of minimum  
692 sequence identities. (D) Number of ISs per IS family in the ISOSDB. Only families with 100 or  
693 more IS elements are shown.

694

695 **Figure 2. IS insertions are abundant in intestinal bacteria.** (A) Abundance of ISs from ITA,  
696 JPN, and MDG individuals. Each data point represents one new insertion not found in the  
697 reference assembly. The y-axis is the relative IS depth percentage (IS depth/ (WT allele depth +  
698 IS depth)). (B) Number of insertions per sample shown in A. (C) IS insertions per bacterial class.  
699 The intensity of each bar is proportional to the number of IS insertions. (D) IS insertions in  
700 *Bacteroidia* and *Clostridia* bacteria organized by IS family. The intensity of each bar is  
701 proportional to the number of IS insertions. (E) Preferential IS insertion in either intergenic (left  
702 side, red) or intragenic (right side, blue) loci for highly abundant ISs (paired T test with FDR  
703 multiple testing correction, maximum adjusted  $p$  value = 0.05). The difference between  
704 intragenic and intergenic insertions individual IS elements was averaged between multiple  
705 individuals and is shown on the X axis.

706

707 **Figure 3. IS insertions are commonly found in bacterial accessory genes.** (A) Number of  
708 shared and unique iORFs within ITA, JPN, and MDG individuals. (B) Heatmap of IS insertions in  
709 different gene functional categories. (C) Statistically significant enrichment of ISs in the  
710 functional categories from B. White asterisks represent categories where the iORFs are over-  
711 abundant compared to all genes and blue asterisks represent categories where the iORFs are  
712 under-abundant compared to all genes (Fisher's exact test with FDR multiple comparison  
713 correction,  $***p < 10^{-24}$ ,  $**p < 10^{-3}$ ,  $*p < 0.05$ ). (D) Location and relative IS depth in shared  
714 iORFs. The location of the insertion (either above or below the gene representation) is  
715 representative of the study. (E-F) Number of IS insertions in iORFs in the functional categories

716 in B from different bacterial classes (E) and IS families (F). (G) Rate of IS insertions in  
717 transposases. Rectangles in the red dashed line are self-targets and rectangles outside of the  
718 red dashed line are non-synonymous-targets.

719

720 **Figure 4. ISOSDB412 insertion in *Bacteroides* species replicates findings from intestinal**

721 **metagenomic data.** (A and D) Representative IS-Seq deep sequencing of ISOSDB412

722 insertions in *Bt* (A) and *Bf* (D). (B and E) Functional enrichment of ISOSDB412 insertions in *Bt*

723 (B) and *Bf* (E) (Fisher's exact test, \* $p < 0.06$ , \*\*\* $p < 0.001$ ). (C and F) ISOSDB412 insertions

724 were counted in intergenic and intragenic loci in *Bt* (C) and *Bf* (F) (paired T-test, \* $p < 0.05$ ). (G)

725 Representative IS-Seq of ISOSDB412 insertions of *Bt* passaged in either BHIS or MM. (H)

726 Number of ISOSDB412 insertions in each condition in G (paired T test). (I) Number of

727 ISOSDB412 insertions in EPS biogenesis genes in G (paired T test). (J) Representative IS-Seq

728 of ISOSDB412 insertions of *Bt* chronically infected with DAC15 or DAC17. (K) Number of

729 ISOSDB412 insertions in each condition in J (unpaired T test, \* $p < 0.05$ ). (L) Number of

730 ISOSDB412 insertions in EPS biogenesis genes in J (unpaired T test, \* $p < 0.05$ ).

731

732 **Figure 5. IS insertions are maintained in the intestinal microbiota for extended time**

733 **periods.** (A) IS insertions are depicted as rectangles, with the color intensity proportional to the

734 relative IS depth percentage. Each insertion is unique based on insertion position and the same

735 insertions are aligned vertically. Orange-colored IS insertions are present at the first timepoint

736 (week 0), green IS insertions are new insertions not present at the initial timepoint, and blue IS

737 insertions are new insertions at timepoints after their first appearance. (B) Number of IS

738 insertions per timepoint for IS families (red) or taxonomic classes (blue). (C) Rate of new IS

739 insertions per week. (D) Dynamics of IS insertions over time for gene functional category iORFs.

740 Data from every individual was used for this figure. The legend for this panel is the same as in  
741 A.

742

743 **Figure 6. FMT transfer of IS insertions between donors and recipients.** (A) Blue rectangles  
744 are IS element insertions in donor samples and red rectangles are IS insertions in recipient  
745 samples. The same insertions in donor and recipients are aligned vertically. Week 0 is the  
746 transplanted fecal material. (B) Heatmap showing new IS insertions that were detected 2 weeks  
747 after transplantation and are detected in both donor and recipient samples (see Fig. S6). (C)  
748 Loss of IS insertions detected in the transplanted fecal material (week 0) from recipients (paired  
749 T test,  $**p < 0.01$ ). (D) Similar rates of new IS insertions are found in both donor and recipients  
750 (unpaired T test. Outliers removed prior to this test using the ROUT method where  $Q = 1\%$ ).

751

752 **Figure 7. Antibiotic treatment and diet intervention alters the IS insertional landscape.**

753 (A) Heatmap showing IS insertion dynamics during antibiotic treatment. Only insertions in alleles  
754 with less than or equal to 200% of the week 0 read depth are shown in this panel. Horizontal  
755 black bars at the 0.6 Week timepoint are present in individuals who did not have an available  
756 sample for this timepoint. (B) Antibiotic treatment significantly decreases the number of IS  
757 insertions present following week 0 (unpaired T test,  $*** p < 0.005$ ). (C) Dynamics of IS  
758 insertions in *susCD/tonB* genes during the diet timecourse. Data from every individual was used  
759 for this figure panel. (D) New *BT1119* IS insertions arise after the diet intervention has ended.  
760 Wild type allele depth is shown as a black line and IS insertion allele depth is shown as a red  
761 bar.

762

763 **Supplemental Tables**

764 **Table S1. IS element families represented in ISOSDB, Related to Figure 1**

765

766 **References**

- 767 1. Shkoporov, A.N., Clooney, A.G., Sutton, T.D.S., Ryan, F.J., Daly, K.M., Nolan, J.A.,  
768 McDonnell, S.A., Khokhlova, E.V., Draper, L.A., Forde, A., et al. (2019). The human gut  
769 virome is highly diverse, stable, and individual specific. *Cell Host Microbe* 26, 527-  
770 541.e525. [10.1016/j.chom.2019.09.009](https://doi.org/10.1016/j.chom.2019.09.009).
- 771 2. Forster, S.C., Liu, J., Kumar, N., Gulliver, E.L., Gould, J.A., Escobar-Zepeda, A.,  
772 Mkandawire, T., Pike, L.J., Shao, Y., Stares, M.D., et al. (2022). Strain-level  
773 characterization of broad host range mobile genetic elements transferring antibiotic  
774 resistance from the human microbiome. *Nat Commun* 13, 1445. [10.1038/s41467-022-  
775 29096-9](https://doi.org/10.1038/s41467-022-29096-9).
- 776 3. Jiang, X., Hall, A.B., Xavier, R.J., and Alm, E.J. (2019). Comprehensive analysis of  
777 chromosomal mobile genetic elements in the gut microbiome reveals phylum-level  
778 niche-adaptive gene pools. *PLoS One* 14, e0223680. [10.1371/journal.pone.0223680](https://doi.org/10.1371/journal.pone.0223680).
- 779 4. Jiang, X., Hall, A.B., Arthur, T.D., Plichta, D.R., Covington, C.T., Poyet, M., Crothers, J.,  
780 Moses, P.L., Tolonen, A.C., Vlamakis, H., et al. (2019). Invertible promoters mediate  
781 bacterial phase variation, antibiotic resistance, and host adaptation in the gut. *Science*  
782 363, 181-187. [10.1126/science.aau5238](https://doi.org/10.1126/science.aau5238).
- 783 5. Desvaux, M., Dalmasso, G., Beyrouthy, R., Barnich, N., Delmas, J., and Bonnet, R.  
784 (2020). Pathogenicity factors of genomic islands in intestinal and extraintestinal  
785 *Escherichia coli*. *Front Microbiol* 11, 2065. [10.3389/fmicb.2020.02065](https://doi.org/10.3389/fmicb.2020.02065).
- 786 6. Groussin, M., Poyet, M., Sistiaga, A., Kearney, S.M., Moniz, K., Noel, M., Hooker, J.,  
787 Gibbons, S.M., Segurel, L., Froment, A., et al. (2021). Elevated rates of horizontal gene

- 788 transfer in the industrialized human microbiome. *Cell* 184, 2053-2067.e2018.  
789 10.1016/j.cell.2021.02.052.
- 790 7. Brito, I.L., Yilmaz, S., Huang, K., Xu, L., Jupiter, S.D., Jenkins, A.P., Naisilisili, W.,  
791 Tamminen, M., Smillie, C.S., Wortman, J.R., et al. (2016). Mobile genes in the human  
792 microbiome are structured from global to individual scales. *Nature* 535, 435-439.  
793 10.1038/nature18927.
- 794 8. Aziz, R.K., Breitbart, M., and Edwards, R.A. (2010). Transposases are the most  
795 abundant, most ubiquitous genes in nature. *Nucleic Acids Res* 38, 4207-4217.  
796 10.1093/nar/gkq140.
- 797 9. Siguier, P., Gourgouyere, E., and Chandler, M. (2014). Bacterial insertion sequences: their  
798 genomic impact and diversity. *FEMS Microbiol Rev* 38, 865-891. 10.1111/1574-  
799 6976.12067.
- 800 10. He, S., Corneloup, A., Guynet, C., Lavatine, L., Caumont-Sarcos, A., Siguier, P., Marty,  
801 B., Dyda, F., Chandler, M., and Ton Hoang, B. (2015). The IS200/IS605 family and "peel  
802 and paste" single-strand transposition mechanism. *Microbiol Spectr* 3.  
803 10.1128/microbiolspec.MDNA3-0039-2014.
- 804 11. Piegu, B., Bire, S., Arensburger, P., and Bigot, Y. (2015). A survey of transposable  
805 element classification systems--a call for a fundamental update to meet the challenge of  
806 their diversity and complexity. *Mol Phylogenet Evol* 86, 90-109.  
807 10.1016/j.ympev.2015.03.009.
- 808 12. Kosek, D., Hickman, A.B., Ghirlando, R., He, S., and Dyda, F. (2021). Structures of  
809 ISCTh4 transpososomes reveal the role of asymmetry in copy-out/paste-in DNA  
810 transposition. *EMBO J* 40, e105666. 10.15252/embj.2020105666.



- 811 13. Jellen-Ritter, A.S., and Kern, W.V. (2001). Enhanced expression of the multidrug efflux  
812 pumps AcrAB and AcrEF associated with insertion element transposition in *Escherichia*  
813 *coli* mutants selected with a fluoroquinolone. *Antimicrob Agents Chemother* **45**, 1467-  
814 1472. [10.1128/aac.45.5.1467-1472.2001](https://doi.org/10.1128/aac.45.5.1467-1472.2001).
- 815 14. Shankar, N., Baghdayan, A.S., and Gilmore, M.S. (2002). Modulation of virulence within  
816 a pathogenicity island in vancomycin-resistant *Enterococcus faecalis*. *Nature* **417**, 746-  
817 750. [10.1038/nature00802](https://doi.org/10.1038/nature00802).
- 818 15. Chain, P.S., Carniel, E., Larimer, F.W., Lamerdin, J., Stoutland, P.O., Regala, W.M.,  
819 Georgescu, A.M., Vergez, L.M., Land, M.L., Motin, V.L., et al. (2004). Insights into the  
820 evolution of *Yersinia pestis* through whole-genome comparison with *Yersinia*  
821 *pseudotuberculosis*. *Proc Natl Acad Sci U S A* **101**, 13826-13831.  
822 [10.1073/pnas.0404012101](https://doi.org/10.1073/pnas.0404012101).
- 823 16. Manson, J.M., Hancock, L.E., and Gilmore, M.S. (2010). Mechanism of chromosomal  
824 transfer of *Enterococcus faecalis* pathogenicity island, capsule, antimicrobial resistance,  
825 and other traits. *Proc Natl Acad Sci U S A* **107**, 12269-12274.  
826 [10.1073/pnas.1000139107](https://doi.org/10.1073/pnas.1000139107).
- 827 17. Hawkey, J., Monk, J.M., Billman-Jacobe, H., Palsson, B., and Holt, K.E. (2020). Impact  
828 of insertion sequences on convergent evolution of *Shigella* species. *PLoS Genet* **16**,  
829 e1008931. [10.1371/journal.pgen.1008931](https://doi.org/10.1371/journal.pgen.1008931).
- 830 18. Leavis, H.L., Willems, R.J., van Wamel, W.J., Schuren, F.H., Caspers, M.P., and  
831 Bonten, M.J. (2007). Insertion sequence-driven diversification creates a globally  
832 dispersed emerging multiresistant subspecies of *E. faecium*. *PLoS Pathog* **3**, e7.  
833 [10.1371/journal.ppat.0030007](https://doi.org/10.1371/journal.ppat.0030007).

- 834 19. Kirsch, J.M., Ely, S., Stellfox, M.E., Hullahalli, K., Luong, P., Palmer, K.L., Van Tyne, D.,  
835 and Duerkop, B.A. (2023). Targeted IS-element sequencing uncovers transposition  
836 dynamics during selective pressure in enterococci. *PLoS Pathog* 19, e1011424.  
837 10.1371/journal.ppat.1011424.
- 838 20. Zlitni, S., Bishara, A., Moss, E.L., Tkachenko, E., Kang, J.B., Culver, R.N., Andermann,  
839 T.M., Weng, Z., Wood, C., Handy, C., et al. (2020). Strain-resolved microbiome  
840 sequencing reveals mobile elements that drive bacterial competition on a clinical  
841 timescale. *Genome Med* 12, 50. 10.1186/s13073-020-00747-0.
- 842 21. Zhao, S., Lieberman, T.D., Poyet, M., Kauffman, K.M., Gibbons, S.M., Groussin, M.,  
843 Xavier, R.J., and Alm, E.J. (2019). Adaptive evolution within gut microbiomes of healthy  
844 people. *Cell Host Microbe* 25, 656-667.e658. 10.1016/j.chom.2019.03.007.
- 845 22. Elhenawy, W., Tsai, C.N., and Coombes, B.K. (2019). Host-specific adaptive  
846 diversification of Crohn's disease-associated adherent-invasive *Escherichia coli*. *Cell*  
847 *Host Microbe* 25, 301-312.e305. 10.1016/j.chom.2018.12.010.
- 848 23. Barreto, H.C., Frazão, N., Sousa, A., Konrad, A., and Gordo, I. (2020). Mutation  
849 accumulation and horizontal gene transfer in *Escherichia coli* colonizing the gut of old  
850 mice. *Commun Integr Biol* 13, 89-96. 10.1080/19420889.2020.1783059.
- 851 24. Siguier, P., Perochon, J., Lestrade, L., Mahillon, J., and Chandler, M. (2006). ISfinder:  
852 the reference centre for bacterial insertion sequences. *Nucleic Acids Res* 34, D32-36.  
853 10.1093/nar/gkj014.
- 854 25. Kichenaradja, P., Siguier, P., Pérochon, J., and Chandler, M. (2010). ISbrowser: an  
855 extension of ISfinder for visualizing insertion sequences in prokaryotic genomes. *Nucleic*  
856 *Acids Res* 38, D62-68. 10.1093/nar/gkp947.

- 857 26. Gounot, J.S., Chia, M., Bertrand, D., Saw, W.Y., Ravikrishnan, A., Low, A., Ding, Y., Ng,  
858 A.H.Q., Tan, L.W.L., Teo, Y.Y., et al. (2022). Genome-centric analysis of short and long  
859 read metagenomes reveals uncharacterized microbiome diversity in Southeast Asians.  
860 Nat Commun 13, 6044. 10.1038/s41467-022-33782-z.
- 861 27. Robinson, D.G., Lee, M.C., and Marx, C.J. (2012). OASIS: an automated program for  
862 global investigation of bacterial and archaeal insertion sequences. Nucleic Acids Res 40,  
863 e174. 10.1093/nar/gks778.
- 864 28. Tempel, S., Bedo, J., and Talla, E. (2022). From a large-scale genomic analysis of  
865 insertion sequences to insights into their regulatory roles in prokaryotes. BMC Genomics  
866 23, 451. 10.1186/s12864-022-08678-3.
- 867 29. Nzabarushimana, E., and Tang, H. (2018). Insertion sequence elements-mediated  
868 structural variations in bacterial genomes. Mob DNA 9, 29. 10.1186/s13100-018-0134-3.
- 869 30. Quadrana, L., Bortolini Silveira, A., Mayhew, G.F., LeBlanc, C., Martienssen, R.A.,  
870 Jeddelloh, J.A., and Colot, V. (2016). The *Arabidopsis thaliana* mobilome and its impact  
871 at the species level. Elife 5, e15716. 10.7554/eLife.15716.
- 872 31. Hawkey, J., Hamidian, M., Wick, R.R., Edwards, D.J., Billman-Jacobe, H., Hall, R.M.,  
873 and Holt, K.E. (2015). ISMapper: identifying transposase insertion sites in bacterial  
874 genomes from short read sequence data. BMC Genomics 16, 667. 10.1186/s12864-015-  
875 1860-2.
- 876 32. Durrant, M.G., Li, M.M., Siranosian, B.A., Montgomery, S.B., and Bhatt, A.S. (2020). A  
877 bioinformatic analysis of integrative mobile genetic elements highlights their role in  
878 bacterial adaptation. Cell Host Microbe 27, 140-153.e149. 10.1016/j.chom.2019.10.022.

- 879 33. Sheng, Y., Wang, H., Ou, Y., Wu, Y., Ding, W., Tao, M., Lin, S., Deng, Z., Bai, L., and  
880 Kang, Q. (2023). Insertion sequence transposition inactivates CRISPR-Cas immunity.  
881 Nat Commun 14, 4366. 10.1038/s41467-023-39964-7.
- 882 34. Rampelli, S., Soverini, M., D'Amico, F., Barone, M., Tavella, T., Monti, D., Capri, M.,  
883 Astolfi, A., Brigidi, P., Biagi, E., et al. (2020). Shotgun metagenomics of gut microbiota in  
884 humans with up to extreme longevity and the increasing role of xenobiotic degradation.  
885 mSystems 5. 10.1128/mSystems.00124-20.
- 886 35. Yachida, S., Mizutani, S., Shiroma, H., Shiba, S., Nakajima, T., Sakamoto, T.,  
887 Watanabe, H., Masuda, K., Nishimoto, Y., Kubo, M., et al. (2019). Metagenomic and  
888 metabolomic analyses reveal distinct stage-specific phenotypes of the gut microbiota in  
889 colorectal cancer. Nat Med 25, 968-976. 10.1038/s41591-019-0458-7.
- 890 36. Pasolli, E., Asnicar, F., Manara, S., Zolfo, M., Karcher, N., Armanini, F., Beghini, F.,  
891 Manghi, P., Tett, A., Ghensi, P., et al. (2019). Extensive unexplored human microbiome  
892 diversity revealed by over 150,000 genomes from metagenomes spanning age,  
893 geography, and lifestyle. Cell 176, 649-662.e620. 10.1016/j.cell.2019.01.001.
- 894 37. Rinninella, E., Raoul, P., Cintoni, M., Franceschi, F., Miggiano, G.A.D., Gasbarrini, A.,  
895 and Mele, M.C. (2019). What is the healthy gut microbiota composition? A changing  
896 ecosystem across age, environment, diet, and diseases. Microorganisms 7.  
897 10.3390/microorganisms7010014.
- 898 38. Alpizar-Rodriguez, D., Lesker, T.R., Gronow, A., Gilbert, B., Raemy, E., Lamacchia, C.,  
899 Gabay, C., Finckh, A., and Strowig, T. (2019). *Prevotella copri* in individuals at risk for  
900 rheumatoid arthritis. Ann Rheum Dis 78, 590-593. 10.1136/annrheumdis-2018-214514.

- 901 39. Scher, J.U., Szczesnak, A., Longman, R.S., Segata, N., Ubeda, C., Bielski, C., Rostron,  
902 T., Cerundolo, V., Pamer, E.G., Abramson, S.B., et al. (2013). Expansion of intestinal  
903 *Prevotella copri* correlates with enhanced susceptibility to arthritis. *Elife* 2, e01202.  
904 10.7554/eLife.01202.
- 905 40. Hughes, E.R., Winter, M.G., Duerkop, B.A., Spiga, L., Furtado de Carvalho, T., Zhu, W.,  
906 Gillis, C.C., Buttner, L., Smoot, M.P., Behrendt, C.L., et al. (2017). Microbial respiration  
907 and formate oxidation as metabolic signatures of inflammation-associated dysbiosis. *Cell*  
908 *Host Microbe* 21, 208-219. 10.1016/j.chom.2017.01.005.
- 909 41. Conway, T., and Cohen, P.S. (2015). Commensal and pathogenic *Escherichia coli*  
910 metabolism in the gut. *Microbiol Spectr* 3. 10.1128/microbiolspec.MBP-0006-2014.
- 911 42. Lebreton, F., van Schaik, W., McGuire, A.M., Godfrey, P., Griggs, A., Mazumdar, V.,  
912 Corander, J., Cheng, L., Saif, S., Young, S., et al. (2013). Emergence of epidemic  
913 multidrug-resistant *Enterococcus faecium* from animal and commensal strains. *mBio* 4.  
914 10.1128/mBio.00534-13.
- 915 43. McEvoy, C.R., Tsuji, B., Gao, W., Seemann, T., Porter, J.L., Doig, K., Ngo, D., Howden,  
916 B.P., and Stinear, T.P. (2013). Decreased vancomycin susceptibility in *Staphylococcus*  
917 *aureus* caused by IS256 tempering of *WalKR* expression. *Antimicrob Agents Chemother*  
918 57, 3240-3249. 10.1128/AAC.00279-13.
- 919 44. Kozitskaya, S., Cho, S.H., Dietrich, K., Marre, R., Naber, K., and Ziebuhr, W. (2004).  
920 The bacterial insertion sequence element IS256 occurs preferentially in nosocomial  
921 *Staphylococcus epidermidis* isolates: association with biofilm formation and resistance to  
922 aminoglycosides. *Infect Immun* 72, 1210-1215. 10.1128/IAI.72.2.1210-1215.2004.

- 923 45. Martens, E.C., Koropatkin, N.M., Smith, T.J., and Gordon, J.I. (2009). Complex glycan  
924 catabolism by the human gut microbiota: the Bacteroidetes Sus-like paradigm. *J Biol*  
925 *Chem* 284, 24673-24677. 10.1074/jbc.R109.022848.
- 926 46. Noinaj, N., Guillier, M., Barnard, T.J., and Buchanan, S.K. (2010). TonB-dependent  
927 transporters: regulation, structure, and function. *Annu Rev Microbiol* 64, 43-60.  
928 10.1146/annurev.micro.112408.134247.
- 929 47. Yadav, A.K., Espaillet, A., and Cava, F. (2018). Bacterial Strategies to Preserve Cell  
930 Wall Integrity Against Environmental Threats. *Front Microbiol* 9, 2064.  
931 10.3389/fmicb.2018.02064.
- 932 48. Vassallo, C.N., Doering, C.R., Littlehale, M.L., Teodoro, G.I.C., and Laub, M.T. (2022). A  
933 functional selection reveals previously undetected anti-phage defence systems in the *E.*  
934 *coli* pangenome. *Nat Microbiol* 7, 1568-1579. 10.1038/s41564-022-01219-4.
- 935 49. Aravind, L., Iyer, L.M., Leipe, D.D., and Koonin, E.V. (2004). A novel family of P-loop  
936 NTPases with an unusual phyletic distribution and transmembrane segments inserted  
937 within the NTPase domain. *Genome Biol* 5, R30. 10.1186/gb-2004-5-5-r30.
- 938 50. Komano, T. (1999). Shufflons: multiple inversion systems and integrons. *Annu Rev*  
939 *Genet* 33, 171-191. 10.1146/annurev.genet.33.1.171.
- 940 51. Blattner, F.R., Plunkett, G., 3rd, Bloch, C.A., Perna, N.T., Burland, V., Riley, M., Collado-  
941 Vides, J., Glasner, J.D., Rode, C.K., Mayhew, G.F., et al. (1997). The complete genome  
942 sequence of *Escherichia coli* K-12. *Science* 277, 1453-1462.  
943 10.1126/science.277.5331.1453.

- 944 52. Liu, H., Shiver, A.L., Price, M.N., Carlson, H.K., Trotter, V.V., Chen, Y., Escalante, V.,  
945 Ray, J., Hern, K.E., Petzold, C.J., et al. (2021). Functional genetics of human gut  
946 commensal *Bacteroides thetaiotaomicron* reveals metabolic requirements for growth  
947 across environments. *Cell Rep* 34, 108789. 10.1016/j.celrep.2021.108789.
- 948 53. Flowers, S.A., Evans, S.J., Ward, K.M., McInnis, M.G., and Ellingrod, V.L. (2017).  
949 Interaction between atypical antipsychotics and the gut microbiome in a bipolar disease  
950 cohort. *Pharmacotherapy* 37, 261-267. 10.1002/phar.1890.
- 951 54. Maier, L., Pruteanu, M., Kuhn, M., Zeller, G., Telzerow, A., Anderson, E.E., Brochado,  
952 A.R., Fernandez, K.C., Dose, H., Mori, H., et al. (2018). Extensive impact of non-  
953 antibiotic drugs on human gut bacteria. *Nature* 555, 623-628. 10.1038/nature25979.
- 954 55. Ait Chait, Y., Mottawea, W., Tompkins, T.A., and Hammami, R. (2020). Unravelling the  
955 antimicrobial action of antidepressants on gut commensal microbes. *Sci Rep* 10, 17878.  
956 10.1038/s41598-020-74934-9.
- 957 56. Kyono, Y., Ellezian, L., Hu, Y., Eliadis, K., Moy, J., Hirsch, E.B., Federle, M.J., and  
958 Flowers, S.A. (2022). The atypical antipsychotic quetiapine promotes multiple antibiotic  
959 resistance in *Escherichia coli*. *J Bacteriol* 204, e0010222. 10.1128/jb.00102-22.
- 960 57. Tisza, M.J., Smith, D.D.N., Clark, A.E., Youn, J.H., Khil, P.P., and Dekker, J.P. (2023).  
961 Roving methyltransferases generate a mosaic epigenetic landscape and influence  
962 evolution in *Bacteroides fragilis* group. *Nat Commun* 14, 4082. 10.1038/s41467-023-  
963 39892-6.
- 964 58. Dutilh, B.E., Cassman, N., McNair, K., Sanchez, S.E., Silva, G.G., Boling, L., Barr, J.J.,  
965 Speth, D.R., Seguritan, V., Aziz, R.K., et al. (2014). A highly abundant bacteriophage

- 966 discovered in the unknown sequences of human faecal metagenomes. *Nat Commun* 5,  
967 4498. [10.1038/ncomms5498](https://doi.org/10.1038/ncomms5498).
- 968 59. Hryckowian, A.J., Merrill, B.D., Porter, N.T., Van Treuren, W., Nelson, E.J., Garland,  
969 R.A., Russell, D.A., Martens, E.C., and Sonnenburg, J.L. (2020). *Bacteroides*  
970 *thetaiotaomicron*-infecting bacteriophage isolates inform sequence-based host range  
971 predictions. *Cell Host Microbe* 28, 371-379.e375. [10.1016/j.chom.2020.06.011](https://doi.org/10.1016/j.chom.2020.06.011).
- 972 60. Touchon, M., and Rocha, E.P. (2007). Causes of insertion sequences abundance in  
973 prokaryotic genomes. *Mol Biol Evol* 24, 969-981. [10.1093/molbev/msm014](https://doi.org/10.1093/molbev/msm014).
- 974 61. Watson, A.R., Füssel, J., Veseli, I., DeLongchamp, J.Z., Silva, M., Trigodet, F., Lolans,  
975 K., Shaiber, A., Fogarty, E., Runde, J.M., et al. (2023). Metabolic independence drives  
976 gut microbial colonization and resilience in health and disease. *Genome Biol* 24, 78.  
977 [10.1186/s13059-023-02924-x](https://doi.org/10.1186/s13059-023-02924-x).
- 978 62. Lloyd-Price, J., Arze, C., Ananthakrishnan, A.N., Schirmer, M., Avila-Pacheco, J., Poon,  
979 T.W., Andrews, E., Ajami, N.J., Bonham, K.S., Brislawn, C.J., et al. (2019). Multi-omics  
980 of the gut microbial ecosystem in inflammatory bowel diseases. *Nature* 569, 655-662.  
981 [10.1038/s41586-019-1237-9](https://doi.org/10.1038/s41586-019-1237-9).
- 982 63. Lee, H., Doak, T.G., Popodi, E., Foster, P.L., and Tang, H. (2016). Insertion sequence-  
983 caused large-scale rearrangements in the genome of *Escherichia coli*. *Nucleic Acids*  
984 *Res* 44, 7109-7119. [10.1093/nar/gkw647](https://doi.org/10.1093/nar/gkw647).
- 985 64. Sousa, A., Bourgard, C., Wahl, L.M., and Gordo, I. (2013). Rates of transposition in  
986 *Escherichia coli*. *Biol Lett* 9, 20130838. [10.1098/rsbl.2013.0838](https://doi.org/10.1098/rsbl.2013.0838).



- 987 65. Consuegra, J., Gaffe, J., Lenski, R.E., Hindre, T., Barrick, J.E., Tenaillon, O., and  
988 Schneider, D. (2021). Insertion-sequence-mediated mutations both promote and  
989 constrain evolvability during a long-term experiment with bacteria. *Nat Commun* 12, 980.  
990 10.1038/s41467-021-21210-7.
- 991 66. Palleja, A., Mikkelsen, K.H., Forslund, S.K., Kashani, A., Allin, K.H., Nielsen, T., Hansen,  
992 T.H., Liang, S., Feng, Q., Zhang, C., et al. (2018). Recovery of gut microbiota of healthy  
993 adults following antibiotic exposure. *Nat Microbiol* 3, 1255-1265. 10.1038/s41564-018-  
994 0257-9.
- 995 67. Louis, S., Tappu, R.M., Damms-Machado, A., Huson, D.H., and Bischoff, S.C. (2016).  
996 Characterization of the gut microbial community of obese patients following a weight-  
997 loss intervention using whole metagenome shotgun sequencing. *PLoS One* 11,  
998 e0149564. 10.1371/journal.pone.0149564.
- 999 68. Bischoff, S.C., Damms-Machado, A., Betz, C., Herpertz, S., Legenbauer, T., Löw, T.,  
1000 Wechsler, J.G., Bischoff, G., Austel, A., and Ellrott, T. (2012). Multicenter evaluation of  
1001 an interdisciplinary 52-week weight loss program for obesity with regard to body weight,  
1002 comorbidities and quality of life--a prospective study. *Int J Obes (Lond)* 36, 614-624.  
1003 10.1038/ijo.2011.107.
- 1004 69. Schloissnig, S., Arumugam, M., Sunagawa, S., Mitreva, M., Tap, J., Zhu, A., Waller, A.,  
1005 Mende, D.R., Kultima, J.R., Martin, J., et al. (2013). Genomic variation landscape of the  
1006 human gut microbiome. *Nature* 493, 45-50. 10.1038/nature11711.
- 1007 70. Chanin, R.B., West, P.T., Park, R.M., Wirbel, J., Green, G.Z.M., Miklos, A.M., Gill, M.O.,  
1008 Hickey, A.S., Brooks, E.F., and Bhatt, A.S. (2023). Intragenic DNA inversions expand  
1009 bacterial coding capacity. *bioRxiv*. 10.1101/2023.03.11.532203.

- 1010 71. Milman, O., Yelin, I., and Kishony, R. (2023). Systematic identification of gene-altering  
1011 programmed inversions across the bacterial domain. *Nucleic Acids Res* *51*, 553-573.  
1012 10.1093/nar/gkac1166.
- 1013 72. Pedersen, T.K., Brown, E.M., Plichta, D.R., Johansen, J., Twardus, S.W., Delorey, T.M.,  
1014 Lau, H., Vlamakis, H., Moon, J.J., Xavier, R.J., and Graham, D.B. (2022). The CD4(+) T  
1015 cell response to a commensal-derived epitope transitions from a tolerant to an  
1016 inflammatory state in Crohn's disease. *Immunity* *55*, 1909-1923.e1906.  
1017 10.1016/j.immuni.2022.08.016.
- 1018 73. De Filippo, C., Cavalieri, D., Di Paola, M., Ramazzotti, M., Poullet, J.B., Massart, S.,  
1019 Collini, S., Pieraccini, G., and Lionetti, P. (2010). Impact of diet in shaping gut microbiota  
1020 revealed by a comparative study in children from Europe and rural Africa. *Proc Natl*  
1021 *Acad Sci U S A* *107*, 14691-14696. 10.1073/pnas.1005963107.
- 1022 74. Golden, C.D., Anjaranirina, E.J.G., Fernald, L.C.H., Hartl, D.L., Kremen, C., Milner, D.A.,  
1023 Jr., Ralalason, D.H., Ramihantaniarivo, H., Randriamady, H., Rice, B.L., et al. (2017).  
1024 Cohort Profile: The Madagascar Health and Environmental Research (MAHERY) study  
1025 in north-eastern Madagascar. *Int J Epidemiol* *46*, 1747-1748d. 10.1093/ije/dyx071.
- 1026 75. Carter, M.M., Olm, M.R., Merrill, B.D., Dahan, D., Tripathi, S., Spencer, S.P., Yu, F.B.,  
1027 Jain, S., Neff, N., Jha, A.R., et al. (2023). Ultra-deep sequencing of Hadza hunter-  
1028 gatherers recovers vanishing gut microbes. *Cell* *186*, 3111-3124.e3113.  
1029 10.1016/j.cell.2023.05.046.
- 1030 76. Rasmussen, J.L., Odelson, D.A., and Macrina, F.L. (1986). Complete nucleotide  
1031 sequence and transcription of *ermF*, a macrolide-lincosamide-streptogramin B

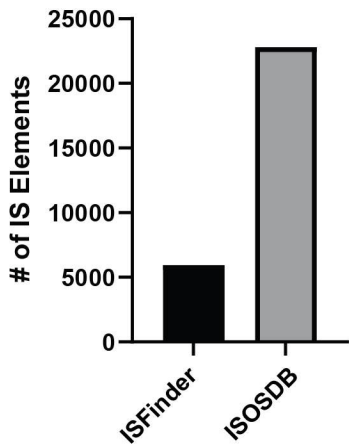
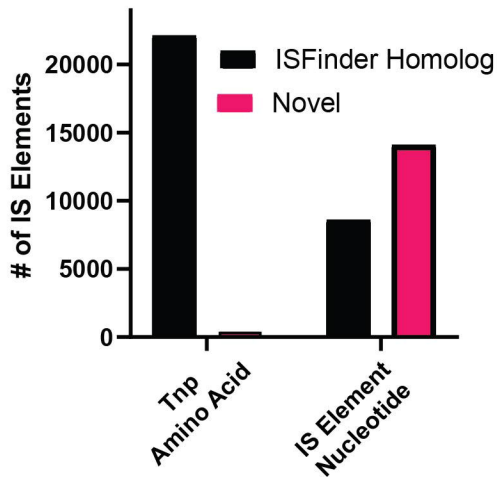
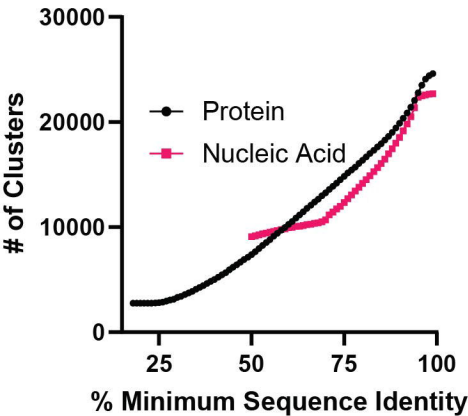
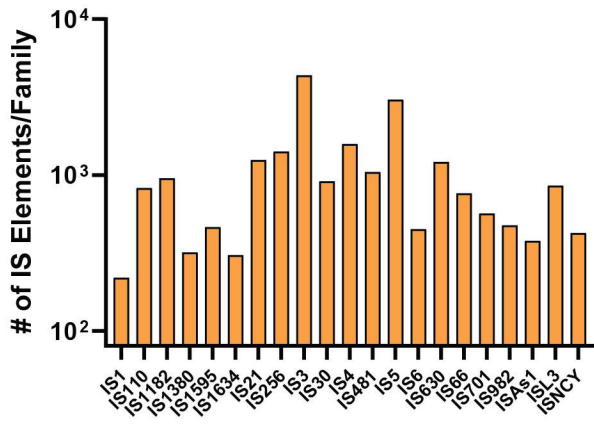
- 1032 resistance determinant from *Bacteroides fragilis*. *J Bacteriol* 168, 523-533.  
1033 10.1128/jb.168.2.523-533.1986.
- 1034 77. Garud, N.R., Good, B.H., Hallatschek, O., and Pollard, K.S. (2019). Evolutionary  
1035 dynamics of bacteria in the gut microbiome within and across hosts. *PLoS Biol* 17,  
1036 e3000102. 10.1371/journal.pbio.3000102.
- 1037 78. Wilson, B.C., Vatanen, T., Jayasinghe, T.N., Leong, K.S.W., Derraik, J.G.B., Albert,  
1038 B.B., Chiavaroli, V., Svirskis, D.M., Beck, K.L., Conlon, C.A., et al. (2021). Strain  
1039 engraftment competition and functional augmentation in a multi-donor fecal microbiota  
1040 transplantation trial for obesity. *Microbiome* 9, 107. 10.1186/s40168-021-01060-7.
- 1041 79. Li, S.S., Zhu, A., Benes, V., Costea, P.I., Hercog, R., Hildebrand, F., Huerta-Cepas, J.,  
1042 Nieuwdorp, M., Salojärvi, J., Voigt, A.Y., et al. (2016). Durable coexistence of donor and  
1043 recipient strains after fecal microbiota transplantation. *Science* 352, 586-589.  
1044 10.1126/science.aad8852.
- 1045 80. Smillie, C.S., Sauk, J., Gevers, D., Friedman, J., Sung, J., Youngster, I., Hohmann, E.L.,  
1046 Staley, C., Khoruts, A., Sadowsky, M.J., et al. (2018). Strain tracking reveals the  
1047 determinants of bacterial engraftment in the human gut following fecal microbiota  
1048 transplantation. *Cell Host Microbe* 23, 229-240.e225. 10.1016/j.chom.2018.01.003.
- 1049 81. Ng, K.M., Aranda-Díaz, A., Tropini, C., Frankel, M.R., Van Treuren, W., O'Loughlin, C.T.,  
1050 Merrill, B.D., Yu, F.B., Pruss, K.M., Oliveira, R.A., et al. (2019). Recovery of the gut  
1051 microbiota after antibiotics depends on host diet, community context, and environmental  
1052 reservoirs. *Cell Host Microbe* 26, 650-665.e654. 10.1016/j.chom.2019.10.011.
- 1053 82. Roodgar, M., Good, B.H., Garud, N.R., Martis, S., Avula, M., Zhou, W., Lancaster, S.M.,  
1054 Lee, H., Babveyh, A., Nesamoney, S., et al. (2021). Longitudinal linked-read sequencing

- 1055 reveals ecological and evolutionary responses of a human gut microbiome during  
1056 antibiotic treatment. *Genome Res* 31, 1433-1446. 10.1101/gr.265058.120.
- 1057 83. Truong, D.T., Tett, A., Pasolli, E., Huttenhower, C., and Segata, N. (2017). Microbial  
1058 strain-level population structure and genetic diversity from metagenomes. *Genome Res*  
1059 27, 626-638. 10.1101/gr.216242.116.
- 1060 84. Bacic, M.K., and Smith, C.J. (2008). Laboratory maintenance and cultivation of  
1061 *Bacteroides* species. *Curr Protoc Microbiol Chapter 13*, Unit 13C.11.  
1062 10.1002/9780471729259.mc13c01s9.
- 1063 85. Hickey, C.A., Kuhn, K.A., Donermeyer, D.L., Porter, N.T., Jin, C., Cameron, E.A., Jung,  
1064 H., Kaiko, G.E., Wegorzewska, M., Malvin, N.P., et al. (2015). Colitogenic *Bacteroides*  
1065 *thetaiotaomicron* antigens access host immune cells in a sulfatase-dependent manner  
1066 via outer membrane vesicles. *Cell Host Microbe* 17, 672-680.  
1067 10.1016/j.chom.2015.04.002.
- 1068 86. Varel, V.H., and Bryant, M.P. (1974). Nutritional features of *Bacteroides fragilis* subsp.  
1069 *fragilis*. *Appl Microbiol* 28, 251-257. 10.1128/am.28.2.251-257.1974.
- 1070 87. Tartera, C., Araujo, R., Michel, T., and Jofre, J. (1992). Culture and decontamination  
1071 methods affecting enumeration of phages infecting *Bacteroides fragilis* in sewage. *Appl*  
1072 *Environ Microbiol* 58, 2670-2673. 10.1128/aem.58.8.2670-2673.1992.
- 1073 88. Lee, M. (2022). bit: a multipurpose collection of bioinformatics tools. *F1000Research*  
1074 11:122. 10.5281/zenodo.3383647.
- 1075 89. Seemann, T. (2014). Prokka: rapid prokaryotic genome annotation. *Bioinformatics* 30,  
1076 2068-2069. 10.1093/bioinformatics/btu153.

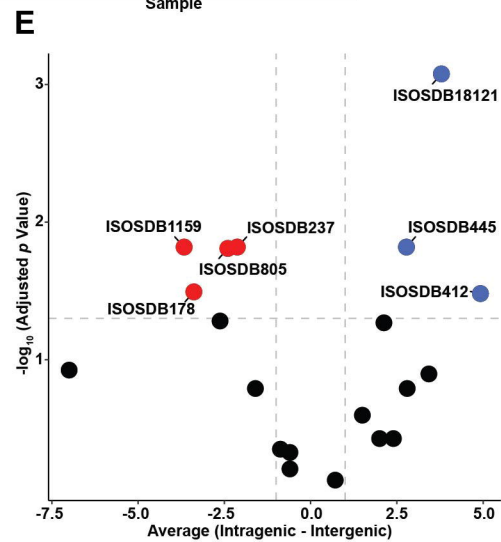
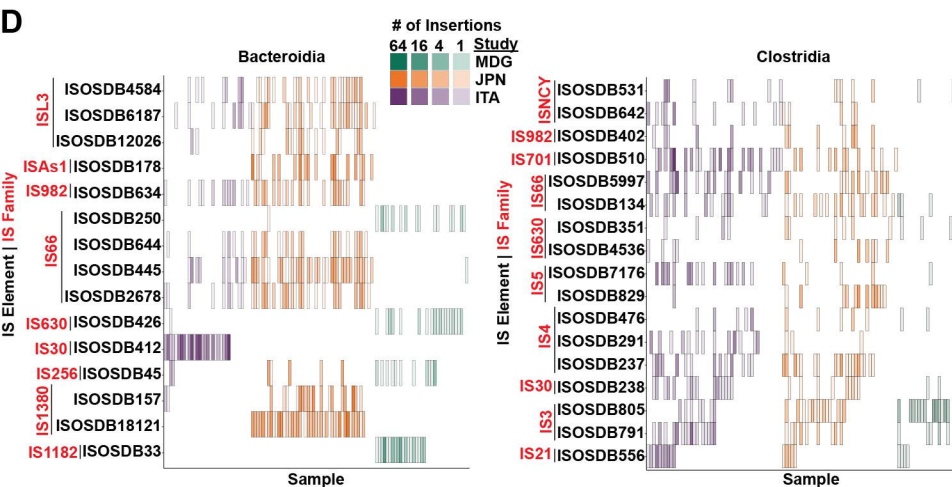
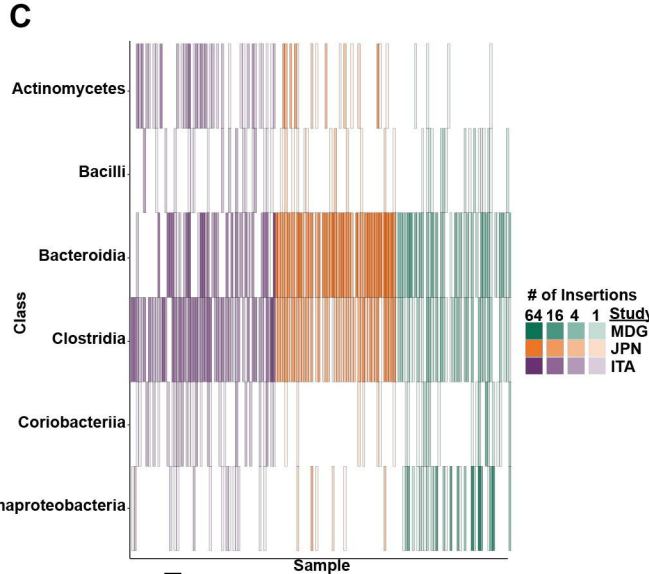
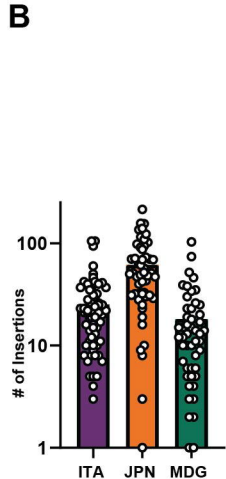
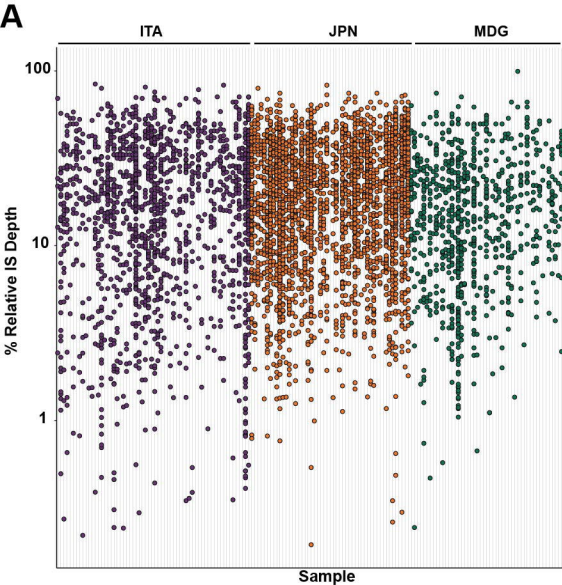
- 1077 90. Li, W., and Godzik, A. (2006). Cd-hit: a fast program for clustering and comparing large  
1078 sets of protein or nucleotide sequences. *Bioinformatics* 22, 1658-1659.  
1079 10.1093/bioinformatics/btl158.
- 1080 91. Altschul, S.F., Gish, W., Miller, W., Myers, E.W., and Lipman, D.J. (1990). Basic local  
1081 alignment search tool. *J Mol Biol* 215, 403-410. 10.1016/s0022-2836(05)80360-2.
- 1082 92. Zdobnov, E.M., and Apweiler, R. (2001). InterProScan--an integration platform for the  
1083 signature-recognition methods in InterPro. *Bioinformatics* 17, 847-848.  
1084 10.1093/bioinformatics/17.9.847.
- 1085 93. Marchler-Bauer, A., Lu, S., Anderson, J.B., Chitsaz, F., Derbyshire, M.K., DeWeese-  
1086 Scott, C., Fong, J.H., Geer, L.Y., Geer, R.C., Gonzales, N.R., et al. (2011). CDD: a  
1087 Conserved Domain Database for the functional annotation of proteins. *Nucleic Acids*  
1088 *Res* 39, D225-229. 10.1093/nar/gkq1189.
- 1089 94. Steinegger, M., and Söding, J. (2017). MMseqs2 enables sensitive protein sequence  
1090 searching for the analysis of massive data sets. *Nat Biotechnol* 35, 1026-1028.  
1091 10.1038/nbt.3988.
- 1092 95. Leinonen, R., Sugawara, H., and Shumway, M. (2011). The sequence read archive.  
1093 *Nucleic Acids Res* 39, D19-21. 10.1093/nar/gkq1019.
- 1094 96. Bushnell, B. BBTools.
- 1095 97. Li, D., Liu, C.M., Luo, R., Sadakane, K., and Lam, T.W. (2015). MEGAHIT: an ultra-fast  
1096 single-node solution for large and complex metagenomics assembly via succinct de  
1097 Bruijn graph. *Bioinformatics* 31, 1674-1676. 10.1093/bioinformatics/btv033.

- 1098 98. Hyatt, D., Chen, G.L., Locascio, P.F., Land, M.L., Larimer, F.W., and Hauser, L.J.  
1099 (2010). Prodigal: prokaryotic gene recognition and translation initiation site identification.  
1100 BMC Bioinformatics 11, 119. 10.1186/1471-2105-11-119.
- 1101 99. Langmead, B., and Salzberg, S.L. (2012). Fast gapped-read alignment with Bowtie 2.  
1102 Nat Methods 9, 357-359. 10.1038/nmeth.1923.
- 1103 100. Pedersen, B.S., and Quinlan, A.R. (2018). Mosdepth: quick coverage calculation for  
1104 genomes and exomes. Bioinformatics 34, 867-868. 10.1093/bioinformatics/btx699.
- 1105 101. Shen, W., Le, S., Li, Y., and Hu, F. (2016). SeqKit: A cross-platform and ultrafast toolkit  
1106 for FASTA/Q file manipulation. PLoS One 11, e0163962. 10.1371/journal.pone.0163962.
- 1107 102. Li, H., Handsaker, B., Wysoker, A., Fennell, T., Ruan, J., Homer, N., Marth, G.,  
1108 Abecasis, G., and Durbin, R. (2009). The sequence alignment/map format and  
1109 SAMtools. Bioinformatics 25, 2078-2079. 10.1093/bioinformatics/btp352.
- 1110 103. Cantalapiedra, C.P., Hernández-Plaza, A., Letunic, I., Bork, P., and Huerta-Cepas, J.  
1111 (2021). eggNOG-mapper v2: Functional annotation, orthology assignments, and domain  
1112 prediction at the metagenomic scale. Mol Biol Evol 38, 5825-5829.  
1113 10.1093/molbev/msab293.
- 1114 104. Tatusov, R.L., Galperin, M.Y., Natale, D.A., and Koonin, E.V. (2000). The COG  
1115 database: a tool for genome-scale analysis of protein functions and evolution. Nucleic  
1116 Acids Res 28, 33-36. 10.1093/nar/28.1.33.
- 1117 105. Alcock, B.P., Raphenya, A.R., Lau, T.T.Y., Tsang, K.K., Bouchard, M., Edalatmand, A.,  
1118 Huynh, W., Nguyen, A.V., Cheng, A.A., Liu, S., et al. (2020). CARD 2020: antibiotic

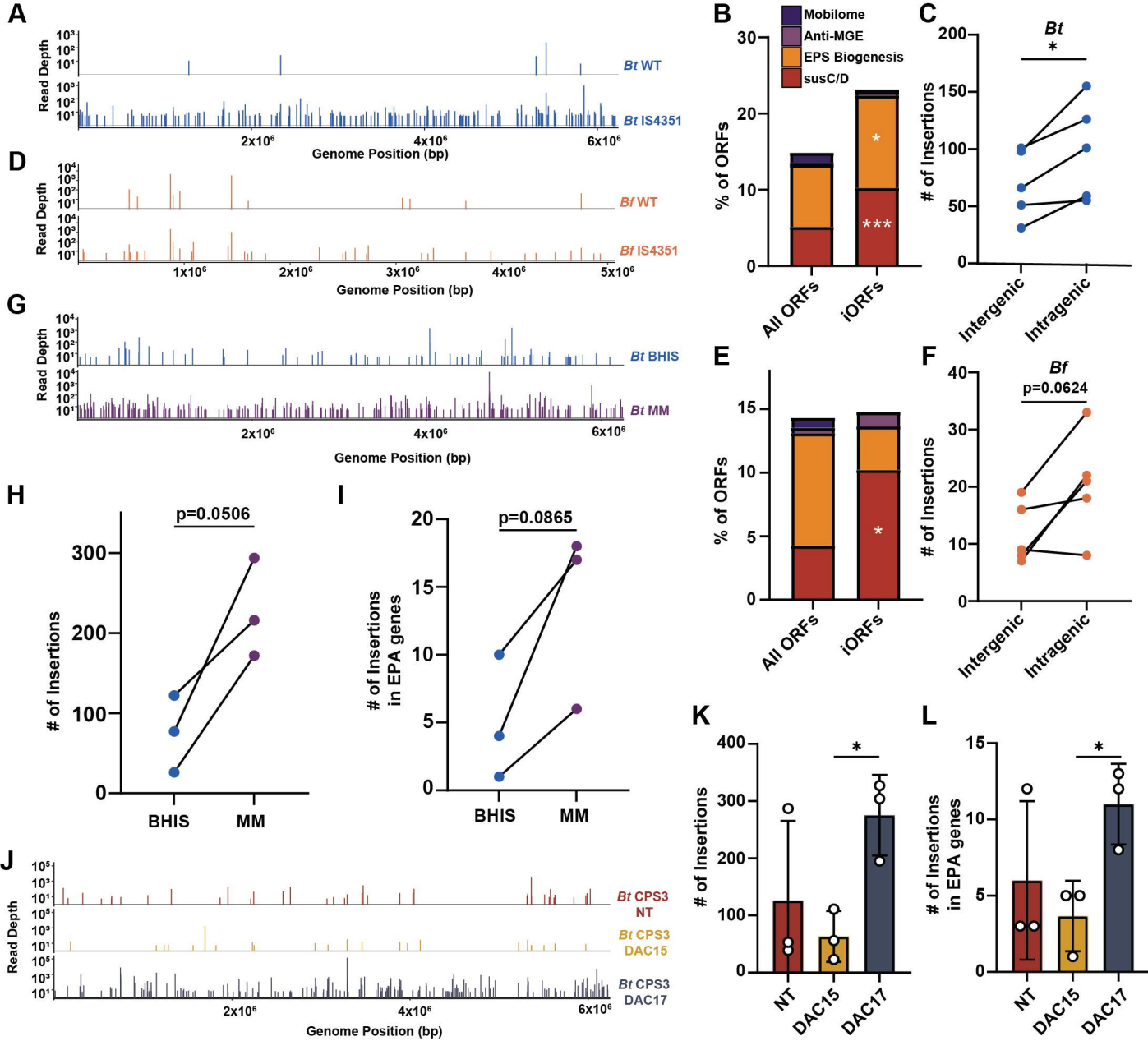
- 1119 resistome surveillance with the comprehensive antibiotic resistance database. *Nucleic*  
1120 *Acids Res* 48, D517-d525. 10.1093/nar/gkz935.
- 1121 106. Wood, D.E., Lu, J., and Langmead, B. (2019). Improved metagenomic analysis with  
1122 Kraken 2. *Genome Biol* 20, 257. 10.1186/s13059-019-1891-0.
- 1123 107. Martin, M. (2011). Cutadapt removes adapter sequences from high-throughput  
1124 sequencing reads. *EMBnetjournal* 17, 3. 10.14806/ej.17.1.200.
- 1125 108. Quinlan, A.R., and Hall, I.M. (2010). BEDTools: a flexible suite of utilities for comparing  
1126 genomic features. *Bioinformatics* 26, 841-842. 10.1093/bioinformatics/btq033.
- 1127 109. Zheng, L., Tan, Y., Hu, Y., Shen, J., Qu, Z., Chen, X., Ho, C.L., Leung, E.L., Zhao, W.,  
1128 and Dai, L. (2022). CRISPR/Cas-Based genome editing for human gut commensal  
1129 *Bacteroides* species. *ACS Synth Biol* 11, 464-472. 10.1021/acssynbio.1c00543.
- 1130 110. Willett, J.L.E., Ji, M.M., and Dunny, G.M. (2019). Exploiting biofilm phenotypes for  
1131 functional characterization of hypothetical genes in *Enterococcus faecalis*. *NPJ Biofilms*  
1132 *Microbiomes* 5, 23. 10.1038/s41522-019-0099-0.
- 1133 111. Jones, K.R., Belvin, B.R., Macrina, F.L., and Lewis, J.P. (2020). Sequence and  
1134 characterization of shuttle vectors for molecular cloning in *Porphyromonas*, *Bacteroides*  
1135 and related bacteria. *Mol Oral Microbiol* 35, 181-191. 10.1111/omi.12304.
- 1136
- 1137
- 1138

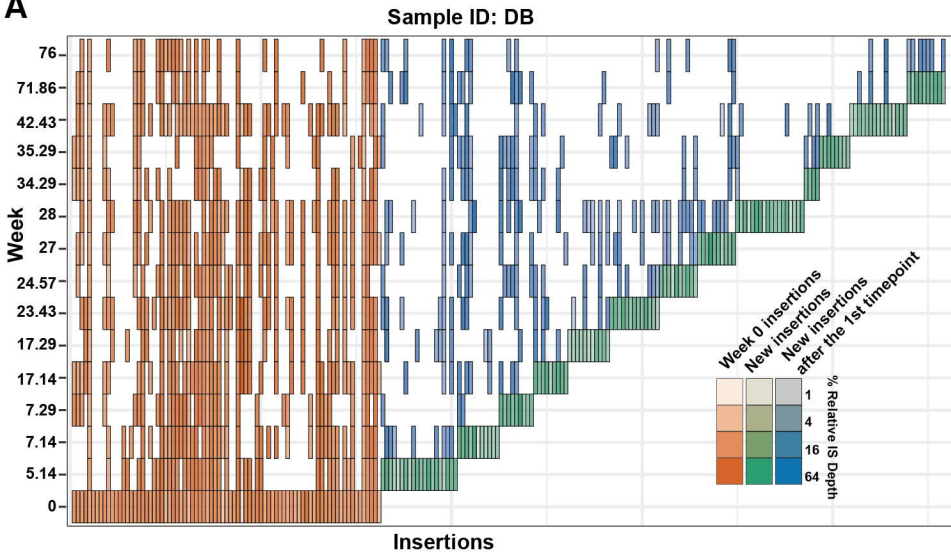
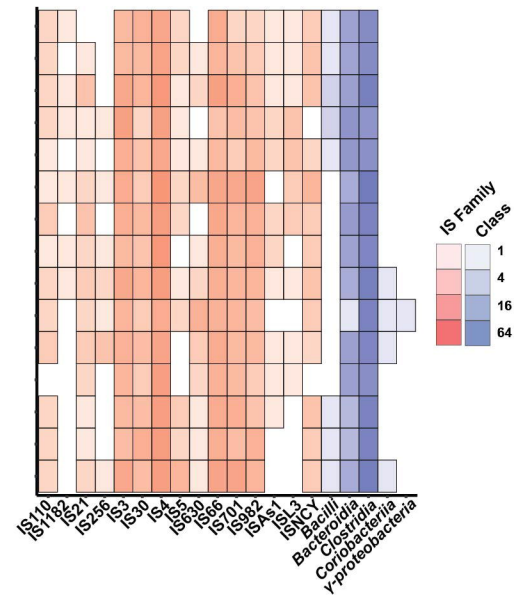
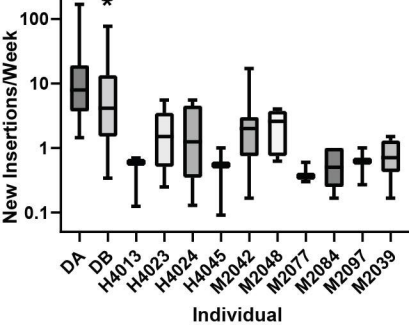
**A****B****C****D**









**A****B****C****D**